"ROLE OF MAGNETIC RESONANACE IMAGING IN EVALUATION OF EXTENT AND ETIOLOGICAL FACTORS IN COMPRESSIVE MYELOPATHY"

By

Dr. ANUSHA REDDY B.

DISSERTATION SUBMITTED TO SRI DEVARAJ URS ACADEMY OF HIGHER EDUCATION AND RESEARCH, KOLAR, KARNATAKA

In partial fulfillment of the requirements for the degree of

DOCTOR OF MEDICINE
IN
RADIODIAGNOSIS

Under the Guidance of

Dr. PURNIMA HEGDE, MD,
PROFESSOR & HOD, RADIODIAGNOSIS

DEPARTMENT OF RADIODIAGNOSIS,
SRI DEVARAJ URS MEDICAL COLLEGE,
TAMAKA, KOLAR-563101

MAY 2016

SRI DEVARAJ URS ACADEMY OF HIGHER EDUCATION AND RESEARCH TAMAKA, KOLAR, KARNATAKA

DECLARATION BY THE CANDIDATE

I hereby declare that this dissertation entitled **"ROLE OF MAGNETIC RESONANACE IMAGING IN EVALUATION OF EXTENT AND ETIOLOGICAL FACTORS IN COMPRESSIVE MYELOPATHY"** is a bonafide and genuine research work carried out by me under the guidance of **Dr. PURNIMA HEGDE**, Professor & Head, Department of Radiodiagnosis, Sri Devaraj Urs Medical College, Kolar, in partial fulfillment of University regulation for the award "**M.D. DEGREE IN RADIODIAGNOSIS**", the examination to be held in April, 2016 by SDUAHER. This has not been submitted by me previously for the award of any degree or diploma from the university or any other university.

Dr. ANUSHA REDDY B.
Postgraduate in Radiodiagnosis
Sri Devaraj Urs Medical College
Tamaka
Kolar

Date:
Place: Kolar

SRI DEVARAJ URS ACADEMY OF HIGHER EDUCATION AND RESEARCH TAMAKA, KOLAR, KARNATAKA

CERTIFICATE BY THE GUIDE & HOD

This is to certify that the dissertation entitled "**ROLE OF MAGNETIC RESONANACE IMAGING IN EVALUATION OF EXTENT AND ETIOLOGICAL FACTORS IN COMPRESSIVE MYELOPATHY"** is a bonafide research work done by **Dr. ANUSHA REDDY B.,** under my direct guidance and supervision at Sri Devaraj Urs Medical College, Kolar**,** in partial fulfillment of the requirement for the degree of "**M.D. IN RADIODIAGNOSIS"**.

Dr. PURNIMA HEGDE, MD
Professor&HOD
Department Of Radiodiagnosis
Sri Devaraj Urs Medical College,
Tamaka
Kolar

Date:

Place: Kolar

SRI DEVARAJ URS ACADEMY OF HIGHER EDUCATION AND RESEARCH TAMAKA, KOLAR, KARNATAKA

ENDORSEMENT BY THE HEAD OF THE DEPARTMENT AND PRINCIPAL

This is to certify that the dissertation entitled **"ROLE OF MAGNETIC RESONANACE IMAGING IN EVALUATION OF EXTENT AND ETIOLOGICAL FACTORS IN COMPRESSIVE MYELOPATHY"** is a bonafide research work done by **Dr. ANUSHA REDDY B.** under the direct guidance and supervision of **Dr. PURNIMA HEGDE,** Professor & Head, Department of Radiodiagnosis, Sri Devaraj Urs Medical College, Kolar, in partial fulfillment of University regulation for the award "**M.D. DEGREE IN RADIODIAGNOSIS**".

Dr. PURNIMA HEGDE MD,
Professor & HOD
Department Of Radiodiagnosis,
Sri Devaraj Urs Medical College,
Tamaka, Kolar

Date:
Place: Kolar

Dr. RANGANATH. B. G.
Principal,
Sri Devaraj Urs Medical College,
Tamaka, Kolar

Date:
Place: Kolar

SRI DEVARAJ URS ACADEMY OF HIGHER EDUCATION AND RESEARCH TAMAKA, KOLAR, KARNATAKA

ETHICAL COMMITTEE CERTIFICATE

This is to certify that the Ethical committee of Sri Devaraj Urs Medical College, Tamaka, and Kolar has unanimously approved

Dr. ANUSHA REDDY B.

Post-Graduate student in the subject of

RADIODIAGNOSIS at Sri Devaraj Urs Medical College, Kolar

to take up the Dissertation work entitled

"ROLE OF MAGNETIC RESONANACE IMAGING IN EVALUATION OF EXTENT AND ETIOLOGICAL FACTORS IN COMPRESSIVE MYELOPATHY"

to be submitted to the

SRI DEVARAJ URS ACADEMY OF HIGHER EDUCATION AND RESEARCH CENTER, TAMAKA, KOLAR, KARNATAKA,

Member Secretary

Sri Devaraj Urs Medical College,

Kolar–563101

SRI DEVARAJ URS ACADEMY OF HIGHER EDUCATION AND RESEARCH TAMAKA, KOLAR, KARNATAKA

COPY RIGHT

Dr. ANUSHA REDDY B.

Date:

Place: Kolar

ACKNOWLEDGEMENT

I owe debt and gratitude to my parents ***Sri. B.VISHNU VARDHAN REDDY and Smt.SRI LATHA****, along with my sister* ***B.PRANUSHA REDDY*** *for their moral support and constant encouragement during the study.*

With humble gratitude and great respect, I would like to thank my teacher, mentor and guide, ***Dr. PURNIMA HEGDE,*** *Professor and Head, Department of Radiodiagnosis, Sri Devaraj Urs Medical College, Kolar, for her able guidance, constant encouragement, immense help and valuable advices which went a long way in moulding and enabling me to complete this work successfully. Without her initiative and constant encouragement this study would not have been possible. Her vast experience, knowledge, able supervision and valuable advices have served as a constant source of inspiration during the entire course of my study. I would like to express my sincere thanks to* ***Dr. PATTABHIRAMAN V and Dr. ANIL KUMAR SAKALECHA*** *Professors, Department of Radiodiagnosis, Sri Devaraj Urs Medical College for their valuable support, guidance and encouragement throughout the study.*

I would like to thank all my teachers. ***Dr. N. RACHEGOWDA, Dr. KISHORE KUMAR, Dr. NABAKUMAR SINGH, Dr. ASHWATHNARAYANA, Dr. NAGARAJ, Dr. MANJUNATH, Dr. NAVEEN G NAIK, Dr. JAGADISH, Dr. VINAY, Dr. KUKU MARIAM SURESH and Dr. ANIL KUMAR*** *for their constant guidance and encouragement during the study period.*

I am extremely grateful to the patients who volunteered to this study, without them this study would just be a dream.

I am thankful to my fellow ***postgraduates, especially Dr. Shivaprasad G Savagave*** *and* ***Dr. Sujata*** *for having rendered all their co-operation and help to me during my study.*

My sincere thanks to ***Mrs. Veena*** *along with rest of the computer operators.*

I am also thankful to ***Mr. Chandrasehar,, Mr. Aleem, Mr. Mateen, Ms. Niveditha, Mr. Ravi, Mr. Gurumurthy*** *along with other technicians of Department of Radiodiagnosis, RLJH and Research Institute, Kolar for their help.*

Dr. ANUSHA REDDY B

LIST OF ABBREVIATIONS

ADC	*Apparent Diffusion coefficient*
AF	*Annulus Fibrosus*
ALL	*Anterior Longitudinal Ligament*
AP	*Anteroposterior*
ASIA	*American Spinal Injury Association*
C	*Cervical*
CNS	*Central Nervous System*
CSF	*Cerebrospinal Fluid*
CSM	*Cervical spondylotic myelopathy*
CT	*Computed Tomography*
CVJ	*Cranio-vertebral Junction*
DCM	*Degenerative cervical spondylytic myelopathy*
DRG	*Dorsal root ganglion*
DWI	*Diffusion weighted imaging*
EAC	*Extradural arachnoid cyst*
FDA	*Food and Drug Administration*
FND	*Focal neurological deficits*
Gd-DTPA	Diethylenetriamine Penta-Acetic acid
ISL	*Interspinous ligament*
IVD	*Intervertebral Disc*
IVF	*Intervertebral foramen.*
JOA	*Japanese Orthopaedic Association Score*
L	*Lumbar*

LIST OF ABBREVIATIONS

LF	*Ligamentum flavum*
MRI	*Magnetic Resonance Imaging*
NHL	*Non-Hodgkin lymphoma*
NP	*Nucleus Pulposus*
OPLL	*Ossification of the posterior longitudinal ligament*
PLC	*The Posterior Ligamentous Complex*
PLL	*Posterior Longitudinal Ligament*
RAPT	*Ratio of Anteroposterior-to-transverse diameter*
SCC	*Spinal cord compromise*
SE	*Spin-echo*
SEA	*Spinal epidural abscess*
SEM	*Spinal cord epidural metastasis.*
SI	*Signal Intensity*
SSL	*Supraspinous ligament*
STIR	*Short tau inversion recovery*
T	*Thoracic*
T1W	*T1 weighted*
T2W	*T2 weighted*
TB	*Tuberculosis*
TR	*Transverse*

ABSTRACT

Background: Magnetic resonance imaging (MRI) is currently the standard modality for assessing spinal pathologies, especially for evaluation of spinal cord, intervertebral discs and ligaments. MRI may be considered as the mainstay investigation for evaluation of compressive myelopathy.

Aims and Objectives: Evaluation of various causes of compressive myelopathy and characterization of the extent of spinal cord compression on MRI study and to classify the lesions into extradural, intradural and intramedullary based on the location.

Methodology: This descriptive observational study was conducted at R. L. Jalappa Hospital attached to Sri Devaraj URS Medical College over a period of 18 months in 52 patients referred for MRI to department of Radio-diagnosis and diagnosed with compressive myelopathy. Patients underwent MRI of spine with 1.5T MRI scanner (Siemens® Magnetom Avanto®). Dedicated matrix spine coil for cervical, thoracic and lumbar spine has been used for acquisition of images.

Results: Commonest age group was 41 to 60 years with a male-to-female ratio of 2.7:1. Nearly half of the lesions were located in cervical spine (48%) followed by lower thoracic spine (27%). Approximately 85 % of the patients had extradural compression of the spinal cord, followed by intradural extramedullary (13 %) and intramedullary (2 %). Degenerative changes (36%) and trauma (29 %) were common causes of compressive myelopathy. All cases of degenerative changes were seen in cervical spine (n = 19). Cord signal changes were seen in 45 patients including a case of intramedullary tumour. The

mean reduction in ratio of anteroposterior-to-transverse diameter was 28.85 ± 22.8% (mean ± SD) between normal and abnormal segments. MRI is helpful in depicting the changes within the spinal cord, assessing spinal cord lesions, ligamentous injury, and vertebral and paraspinal abnormalities. It also helps differentiate between spinal cord edema, contusion and hemorrhage, in cases of trauma, which may have different prognostic implications.

Conclusion: MR imaging plays an important role in the imaging of spinal cord lesions. Morphological abnormalities, signal changes within the cord and objective measurements all contribute towards complete evaluation of compressive myelopathy.

TABLE OF CONTENTS

LIST OF TABLES

LIST OF FIGURES

INTRODUCTION

Myelopathy is a broad term used to describe pathologic conditions responsible for spinal cord, meningeal, or perimeningeal space damage/dysfunction[1]. Compressive myelopathy commonly occurs as a result of spinal cord compression due to a variety of causes including compression by osteophyte/extruded disc material, disc herniation, extradural masses such as metastatic deposits, neoplasms and trauma[2].

Radiographs and computed tomography (CT) scan have a low sensitivity for identifying traumatic spinal cord lesions. Magnetic resonance imaging (MRI) is the definitive modality in assessing spinal soft tissue injuries, especially in evaluation of spinal cord, intervertebral discs and ligaments. It also helps in identification of spinal cord hemorrhage, contusion and edema, which may have prognostic value[3]. Given that cerebrospinal fluid (CSF), bone, disc, spinal cord and epidural fat show different signal intensity on most sequences, a better spatial resolution can be achieved[4]. MRI also helps best to depict the relation of spinal cord to lesion. It is not surprising that MRI is the mainstay for the evaluation of myelopathy[2].

The purpose of this study is to evaluate the role of MRI in assessing extent and various causes of compressive myelopathy.

AIMS AND OBJECTIVES

- To perform MRI and to evaluate various causes of compressive myelopathy.
- To classify the lesions based on location into extradural, intradural and intramedullary compartments.

REVIEW OF LITERATURE

ANATOMY OF SPINE AND SPINAL CORD

Anatomy of Spinal cord

The spinal cord represents a caudal extension of the medulla oblongata; it terminates in the conus medullaris, typically located at thoracic (T12) or lumbar (L1) level in adults. The cord is slightly flattened along its anterior and posterior surfaces and is enlarged in two regions. The cord widens first for the brachial plexus from cervical (C3) to T2, then for the lumbosacral plexus from T9 to T12. The filum terminale is a slender fibrous strand extending from conus to the coccyx, and cauda equina represents spinal nerve roots extending caudally from the conus within the lumbar subarachnoid space[5].

The three-layered meningeal covering of the central nervous system (CNS) is contiguous with the spinal cord, and all lie within the bony spinal canal. The innermost layer, the piamater, is adherent to the surface of the cord. The middle arachnoid membrane remains closely adherent to the outer layer, the duramater. The space between the arachnoid and piamater is called the subarachnoid space, which contains CSF. This space is contiguous with the intracranial subarachnoid space. A potential space exists between the duramater and arachnoid membrane, called the subdural space. The dentate ligaments are formed by the extension of piamater laterally from the surface of the cord to attach to the duramater, in a saw-tooth fashion, between the exiting nerve roots. The dura extends from the base of the skull to the sacral (S2) level, forming the dural sac, which is surrounded externally by epidural fat and loose connective tissue to fill the remainder of the volume of the bony

spinal canal. The anterior and posterior venous plexuses are also located in the epidural fat[5].

The gray matter of the spinal cord is located internally, in contradistinction to the gray matter of the brain, and is surrounded by white matter tracts; the proportion of gray matter increases in the cervical and lumbar regions. Both dorsal (sensory) and ventral (motor) roots arise along the entire length of the cord and unite to form a total of 31 paired spinal nerves. There are eight cervical, twelve thoracic, five lumbar, and five sacral nerve roots as well as one coccygeal nerve root[5].

Arterial supply to the cord originates from arterial vessels that enter the spinal canal through the neural foramina at all levels of the spinal cord, which are termed radicular branches. Radicular branches arise from the vertebral arteries, the costocervical trunk, and the intercostal and lumbar arteries. The distal branches of the radicular arteries that continue on to supply the cord are termed radiculomedullary arteries, which in the adult are variable in number and position. The radiculomedullary arteries terminate in branches that run cephalocaudal along the surface of the cord, anastomosing with those above and below to form the anterior as well as the paired posterior spinal arteries on the cord surface. The anterior spinal artery provides the major blood supply to the spinal cord, supplying the anterior 70% to 80%, while the posterior spinal arteries supply the posterior 20% to 30%. There are a large number of radiculomedullary arteries supplying the posterior spinal arterial system. Radiculomedullary supply to the anterior spinal artery is more variable and its branches can be divided into three major regions. Two anterior spinal rami from the distal vertebral arteries and radiculomedullary arteries at the C2-3, C5-6, and C8

levels supply the cervical cord. The C5-6 artery is somewhat constant and has been called "the artery to the cervical enlargement." A single radiculomedullary artery, usually located at approximately the T4-5 level, supplies the mid thoracic cord. This represents the smallest territorial division and typically extends from T4 through T8. This area is considered to be most susceptible to ischemic injury[5].

The artery of Adamkiewicz, which arises from a low thoracic or upper lumbar artery, supplies the final thoracolumbar region. This important artery usually arises from a left intercostal branch in the region of T9 to T12. In few people it may arise from a branch at a higher level, but the conus medullaris can be additionally supplied from a lower and smaller radiculomedullary artery. Least often, the artery of Adamkiewicz arises from the upper lumbar arteries[5].

Anatomy of Spine:

The vertebral column forms the central axis of the skeleton and consists of 33 vertebrae. There are seven cervical, twelve thoracic and five lumbar vertebrae (the true, "moveable" vertebrae), and caudally there are five sacral and four coccygeal segments, all of which are fused as the sacrum and coccyx, respectively[6].

The Vertebral Canal

The vertebral canal transmits the spinal cord and, in the lumbar region, the cauda equina. It is formed by the posterior margins of the vertebral bodies and discs anteriorly, and the pedicles and laminae (the neural arch) posteriorly[6].

The Intervertebral Canal (Neural Foramen)

The spinal nerves arise from the spinal cord and leave the spinal canal through the intervertebral canals, each of which is situated between adjacent pedicles. The nerves are accompanied by blood vessels and are supported by extradural fat within each canal[6].

The Ligaments of Vertebral Column

A number of ligaments strengthen the vertebral column. The anterior longitudinal ligament (ALL) runs superoinferiorly between the anterior surfaces of the vertebral bodies from the occiput to the sacrum. The posterior longitudinal ligament (PLL) is applied to the posterior surfaces and narrows as it passes downward. The ligamentum flavum (LF) joins adjacent laminae and the interspinous ligaments (ISL) run between the spinous processes[6].

In the axial plane the ligamentum flavum appears V-shaped and is thickest in the lumbar region. It is the only spinal ligament having elastic properties, increasing in length during flexion. The vertebral column can be considered as a three-column structure. The anterior column is formed by the anterior longitudinal ligament, the anterior annulus fibrosus (AF), and the anterior part of the vertebral body. The middle column comprises the posterior longitudinal ligament, the posterior annulus fibrosus, and the posterior part of the vertebral body. The posterior column consists of the neural arch and posterior ligamentous complex. This concept has implications for spinal stability following trauma[6].

Intervertebral Discs

The intervertebral discs (IVD) lie between the superior and inferior cartilaginous endplates of the adjacent vertebrae, being formed of an outer annulus fibrosus and an inner nucleus pulposus (NP). The IVD functions to provide motion between individual vertebrae and also allows the effective transfer of load[6].

The Craniovertebral Junction and Cervical Vertebral Column

The craniovertebral junction (CVJ) is composed of the occiput, atlas, and axis, and supporting ligaments, enclosing the soft tissues of the medulla, spinal cord, and lower cranial nerves. MRI is the most appropriate means of showing the relationship of bone and soft tissue in this important region. CT demonstrates the bony anatomy. A variety of congenital anomalies of the bony skull base can lead to basilar invagination, when the vertebral column extends into skull base. A similar result, better described as cranial "settling," can occur in the erosive arthropathies due to ligamentous damage. There are seven cervical vertebrae. The atlas vertebra (C1) is a ring of bone with no vertebral body. It articulates superiorly with the occipital condyles of the skull as the atlanto-occipital joints. Think of the Greek myth of Atlas who carried the world on his shoulders and you realize the responsibility of the first vertebra as it carries your "world" or head on your shoulders. The axis vertebra (C2) has a superior extension, the odontoid process (or dens) which represents the body of C1. The anterior arch of C1 is maintained in a fixed position relative to the dens by the transverse ligament, which attaches to the lateral masses of C1. Four joints are formed between C1 and C2, namely the anterior arch of C1 and the dens, the dens and the transverse ligament, and the right and left articular facets. Damage to the ligament,

either by trauma or due to an erosive arthropathy, like rheumatoid arthritis, can result in atlanto-axial subluxation and cervical cord compression. C3 to C6 may be regarded as typical cervical vertebrae. The small, oval vertebral bodies increase in size to C7. The superior projection of each vertebra, the "uncinate process," forms a rim or flange, which indents the posterior–lateral disc and vertebrae above, creating the "uncovertebral joint." The short pedicles extend laterally from the anterior body forming a bridge to the articular pillars, which bear the inferior and superior articular facets. The spinous processes may be bifid and the transverse processes terminate with anterior and posterior tubercles. Each transverse process encloses the foramen transversarium, which transmits the vertebral arteries and veins on each side. C7, the vertebra prominens, has a long, non-bifid spine, and no anterior tubercle on its transverse process. Its foramen transversarium is often small; it only transmits small tributaries of the vertebral vein – the artery enters at C6. The vertebral arteries arise from the subclavian arteries, enter the foramen transversarium of C6, traverse the successive foramina transversaria above this level and enter the skull through the foramen magnum[6].

The Thoracic Vertebral Column

There are 12 thoracic vertebrae distinguished by articulations for the ribs. The vertebral bodies have a slight wedge-shape anteriorly. They also bear demifacets for the ribs on the superior and inferior vertebral bodies. The annulus fibrosus, ALL, and PLL are thickest in this region. The ribs attach at two places: the head of the rib attaches to the vertebrae at the disc and additionally the tubercle of the rib attaches to the transverse process-costotransverse joint. Typically, therefore the ribs arise posteriorly between vertebrae. The first rib articulates only with T1 and similarly the

tenth, eleventh, and twelveth ribs articulate only with T10, T11, and T12 vertebrae. At remaining levels, demi facets superior and inferior to the disc communicate with the head of the rib creating a costovertebral synovial joint. Therefore, the ribs arise posteriorly between vertebrae. In the thoracic region the canal is constant in size and circular in cross-section[6].

The Lumbar Vertebral Column

There are five lumbar vertebrae, the third (L3) being the largest. Lumbar vertebrae have square-shaped anterior vertebral bodies covered by fenestrated cartilage attached to the adjacent discs. Projecting posteriorly are bilateral pedicles composed of thick cortical bone connecting to lamina forming the spinal canal. The articular facets face each other in the sagittal plane, and the transverse distance between the pedicles increases (the interpedicular distance) from L1 to L5. L5 is somewhat atypical with a wedge-shaped body, articulating inferiorly with the sacrum. Not infrequently, it may be fused, wholly or partly, with the body of the sacrum ("sacralization of L5"). Extending from the pedicles is a bony plate called the pars articularis from which extend the superior and inferior articular facets. The posterior superior articular facet of an inferiorly located vertebra connects to the posterior inferior facet of the superior vertebra above creating a diarthrodial synovial lined joint, surrounded by a fibrous capsule posterolaterally with absence of the joint capsule anteriorly, where the ligamentum flavum and synovial membrane are present[6].

MRI ANATOMY OF SPINE

MRI is the primary imaging method for the vertebral column. MRI is ideally suited for the demonstration of soft tissue anatomy of the spinal cord, including vertebral medullary cavity, intervertebral discs, spinal ligaments, spinal cord and its contents and paravertebral musculature. In addition, MRI provides images in multiple planes, does not use ionizing radiation and displays excellent anatomical and pathological information[7].

A typical MRI series will consist of T1 weighted (T1W) and T2 weighted (T2W) sagittal and axial images. Further coronal images and intravenous gadolinium diethylenetriamine pentaacetic acid (Gd-DTPA) contrast administration may be undertaken depending on the clinical picture. The tissue discrimination of MRI is superior to CT. MRI is the only method to show an intrinsic abnormality of the spinal cord substance. On T1W images CSF is dark and, in general, this sequence shows the anatomy. On T2W images CSF appears white and thus there is a myelographic effect. T2W sequences, in general, demonstrate pathology[6].

The Vertebral Body

The vertebral body contains marrow, MRI signal intensity (SI) of which is dependent upon the proportion of red (haemopoietic) and yellow (fatty) marrow, this varying with the age. In the first month of life, the high proportion of red marrow renders the vertebral body hypointense to the intervertebral disc (IVD). Marrow conversion occurs during the first to sixth months, with a progressive increase in T1W signal intensity. In adults, the high proportion of yellow marrow results in the marrow appearing hyperintense to the IVD, particularly in the lumbar region. Focal variations

in marrow SI within the vertebral body are not uncommon. Islands of red marrow or marrow fibrosis appear as areas of reduced T1W and T2W SI. Focal areas of fatty marrow may be seen, particularly around the basivertebral veins. In the elderly, the marrow SI may be very heterogeneous[7].

Intervertebral Discs

The AF is formed by 15-25 laminae of fibrous connective tissue, which due to its fibrous nature appears hypointense on all MRI pulse sequences, particularly T2W images. The AF is attached circumferentially to the periphery of the vertebral body via Sharpey's fibres. The anterior annulus is thicker than the posterior annulus, resulting in the NP lying relatively posteriorly within the IVD. The NP consists of a gel-like substance with approximately 90% of its content being water, rendering it hyperintense on T2W images and of intermediate SI on T1W images. The intranuclear cleft appears as a horizontal band of low SI on sagittal T2W images, which is a normal finding after the age of 30 years[7].

Spinal Ligaments

The spinal ligaments are important stabilizers of the vertebral column and, being made of fibrous tissue, appear as thin black stripes on all MRI pulse sequences. The major ligaments of the cranio-cervical junction include[7]:

- The ligamentum nuchae, which runs from the external occipital protuberance to the posterior arch of the atlas and the cervical spinous processes
- The tectorial membrane, which connects the clivus to the axis, representing the cephalad extension of the PLL

- The transverse atlantal ligament, which connects the posterior dens to the inner margin of the atlas ring
- The alar ligaments, which run between the lateral margins of the dens and the occipital condyles. The ALL and PLL both arise at the skull base and extend continuously downward, attaching to the front and back of the sacrum:
- The ALL runs anterior to the vertebral bodies and discs, being firmly attached to the anterior annulus
- The PLL runs posterior to the vertebral bodies and discs, being wider at the disc space and being firmly attached to the posterior annulus.

The posterior ligamentous complex (PLC) comprises the LF, ISL and supraspinous ligament (SSL)[7]:

- The LF runs between adjacent laminae and the bases of the spinous processes, running laterally in the lumbar region to cover the anterior aspect of the facet joints.
- The ISL runs between the adjacent spinous processes and appears relatively hyperintense, since it is bordered on each side by fat.
- The SSL connects the spinous processes of the thoracic and lumbar vertebrae, terminating between L4 and L5.

  The iliolumbar ligaments arise from the transverse processes of L5 and attach to the posterior iliac crest, helping to stabilize the lumbosacral junction[7].

The Spinal Canal

The spinal canal is divided into the central canal, the lateral recess and the intervertebral foramen (IVF). The boundaries of the central canal are:

- Anteriorly: the vertebral body, IVD and PLL
- Posteriorly: the posterior epidural fat pad, LF and base of the spinous process;

The central canal contains the thecal sac and CSF, the intradural nerve roots and, in the cervical and thoracic region, the spinal cord[7].

The boundaries of the lateral recess are:

- Anteriorly: Vertebral body and IVD
- Medially: Thecal sac
- Laterally: Pedicle, facet joint and IVF
- Posteriorly: the LF and lamina;

The lateral recess contains epidural fat, the traversing nerve root, and epidural vessels[7].

The boundaries of the IVF are:

- Anteriorly: Vertebral body and IVD.
- Posteriorly: LF, pars interarticularis and facet joint.
- Superiorly and inferiorly: Pedicles of the adjacent vertebrae;

IVF contains epidural fat, the exiting nerve root, radicular epidural vessels and sinuvertebral nerves[7].

The Paraspinal Musculature

The paraspinal muscles function to provide stability and allow motion between spinal segments.

The cervical paraspinal muscles may be divided into anterior, lateral and posterior groups:

- Anteriorly: Longus colli and longus capitis
- Laterally: Scalenus anterior, medius and posterior
- Posteriorly: Levator scapulae, splenius capitis, semispinalis capitis and the cervical portion of erector spinae/multifidus.

The thoracic paraspinal muscles include trapezius, semispinalis thoracic, multifidus and erector spinae.

The thoracolumbar muscles are divided into anterior and posterior:

- Anteriorly: psoas major and occasionally psoas minor
- Posteriorly: Multifidus, erector spinae, quadratus lumborum and intertransversarius[7].

MRI Anatomy of Spine

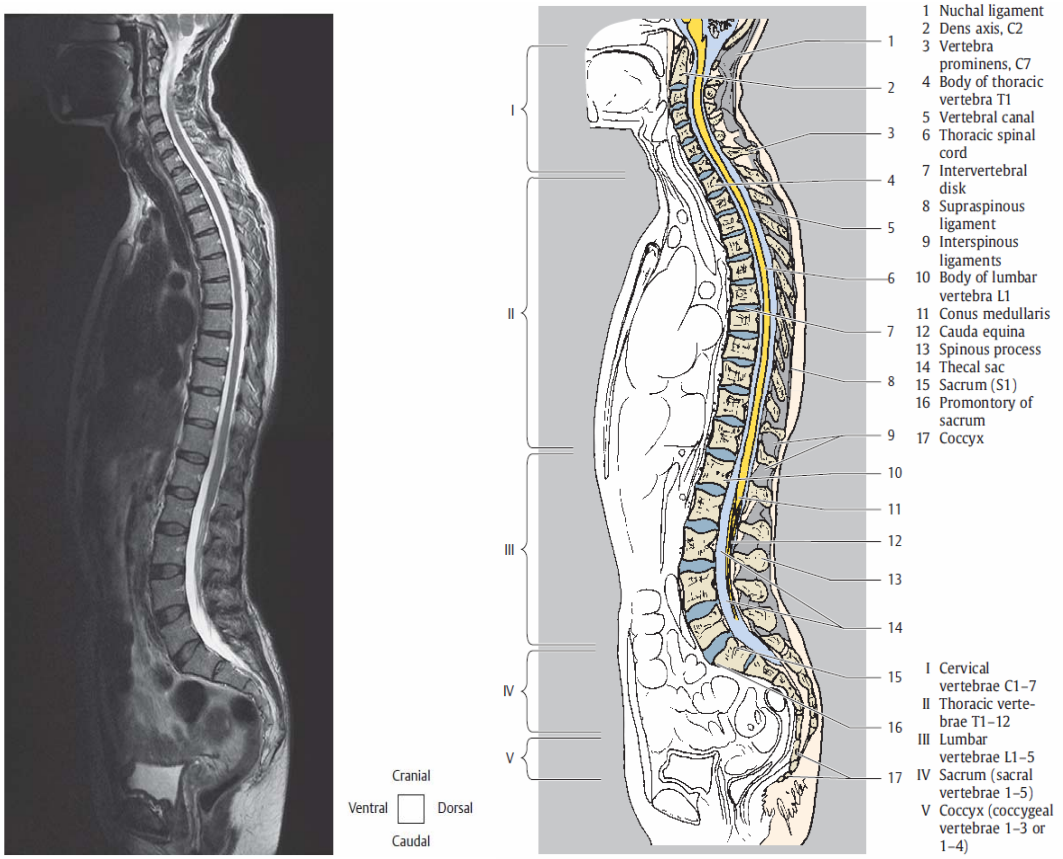

Figure 1. Sagittal T2W image showing whole spine[8]

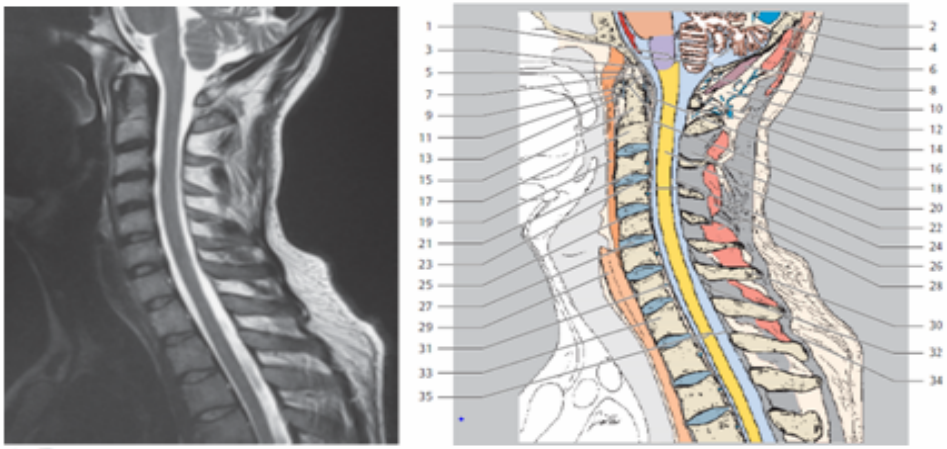

1 Foramen magnum
2 Trapezius muscle (descending part)
3 Tectorial membrane
4 Occipital bone (internal occipital protuberance)
5 Anterior atlanto-occipital membrane
6 Semispinalis capitis muscle
7 Apical ligament of dens
8 Rectus capitis posterior minor muscle
9 Longitudinal fasciculi
10 Posterior atlanto-occipital membrane
11 Atlas (anterior arch)
12 Suboccipital fatty tissue
13 Median atlanto-axial joint
14 Atlas (posterior arch)
15 Axis (dens)
16 Deep cervical veins
17 Axis (vertebral body)
18 Transverse ligament of atlas
19 Longus capitis muscle
20 Posterior longitudinal ligament
21 Inferior vertebral endplate C3
22 Interspinous ligament
23 Superior vertebral endplate C4
24 Cervical spinal cord
25 Anterior longitudinal ligament
26 Premedullary and postmedullary subarachnoid space
27 Intervertebral disk
28 Interspinales muscles
29 Esophagus
30 Spinous process C7
31 Basivertebral veins
32 Ligamentum flavum
33 Thoracic vertebral body T1
34 Supraspinous ligament
35 Bony vertebral canal

Figure 2. Sagittal T2W image through cervical spine[8]

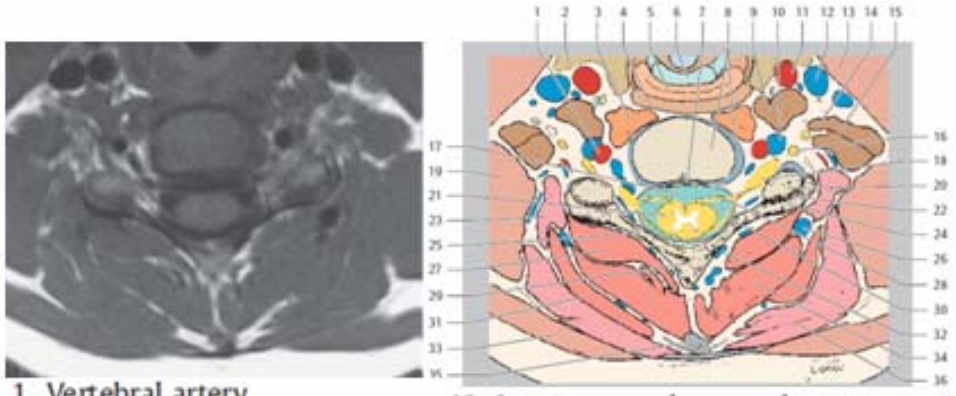

1 Vertebral artery
2 Thyroid gland
3 Longus colli muscle
4 Superior constrictor muscle of pharynx
5 Esophagus
6 Cricoid cartilage
7 Basivertebral veins
8 Cervical vertebral body C5 and intervertebral space C5/C6
9 Scalenus anterior muscle
10 Vertebral vein
11 Common carotid artery
12 Internal jugular vein
13 Sternocleidomastoid muscle
14 Scalenus medius muscle
15 Scalenus posterior muscle
16 Spinal nerve C5
17 Premedullary subarachnoid space
18 Spinal ganglion (nerve root)
19 Levator scapulae muscle
20 Superior articular process
21 Spinal cord
22 Zygapophyseal joint
23 Longissimus cervicis muscle
24 Inferior articular process
25 Posterior vertebral arch C5 (lamina)
26 Deep cervical vein
27 Spinalis cervicis and multifidus muscles
28 Ventral root C6
29 Spinous process
30 Dorsal root C6
31 Semispinalis capitis muscle
32 Posterior external vertebral venous plexus
33 Trapezius muscle
34 Semispinalis cervicis muscle
35 Nuchal ligament
36 Splenius capitis muscle

Figure 3. T2W axial MRI image through C5-6 disc level[8].

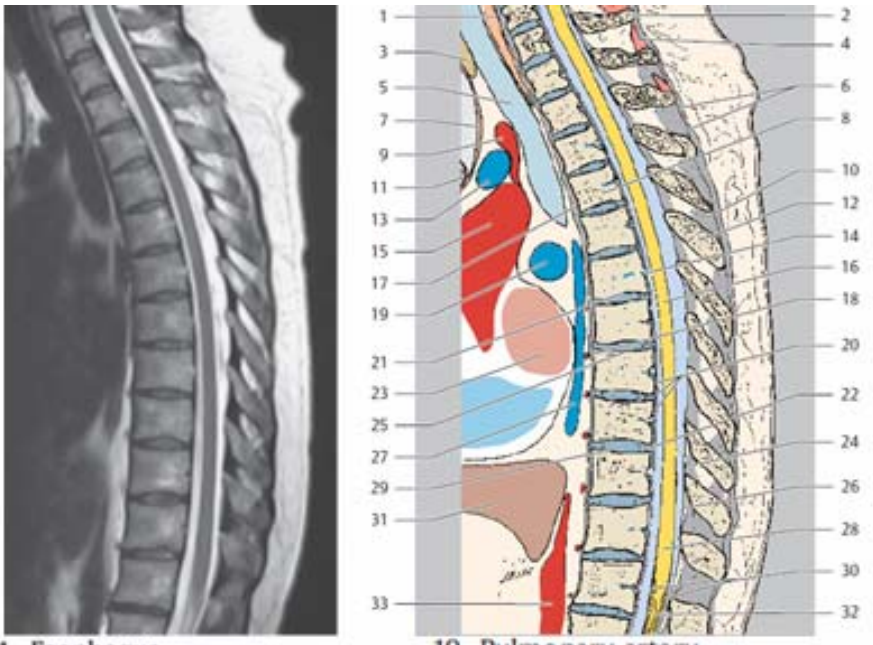

1 Esophagus
2 Vertebra prominens C7
3 Thyroid gland
4 Interspinalis cervicis muscle
5 Trachea
6 Supraspinous ligament
7 Sternohyoid muscle
8 Thoracic vertebral body T4
9 Brachiocephalic trunk
10 Interspinous ligament
11 Sternum (manubrium)
12 Spinous process
13 Left brachiocephalic vein
14 Basivertebral vein
15 Ascending aorta
16 Thoracic spinal cord
17 Anterior longitudinal ligament
18 Posterior intercostal artery
19 Pulmonary artery
20 Posterior longitudinal ligament
21 Inferior vertebral endplate T6
22 Intervertebral disk T9/T10 (anulus fibrosus)
23 Left atrium
24 Ligamentum flavum
25 Superior vertebral endplate T7
26 Epidural fatty tissue (retrospinal fat)
27 Azygos vein
28 Conus medullaris
29 Intervertebral disk T9/T10 (nucleus pulposus)
30 Cauda equina
31 Liver
32 Filum terminale
33 Descending aorta

Figure 4. T2W sagittal image through thoracic cord[8].

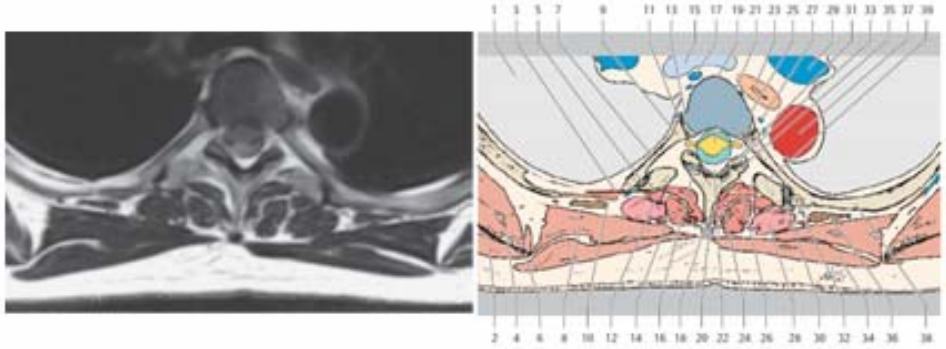

1 Right lung
2 Infraspinatus muscle
3 Intercostal artery
4 Subscapularis muscle
5 Costotransverse joint
6 Scapula
7 Rib (neck)
8 Rhomboid major muscle
9 Fifth rib (head)
10 Intercostal muscles
11 Radiate ligament of head of rib
12 Rotatores thoracis muscles
13 Joint of head of rib
14 Semispinalis thoracis muscle
15 Trachea (bifurcation)
16 Zygapophyseal joint T4/T5
17 Azygos vein
18 Spinous process
19 Intervertebral disk T4/T5
20 Supraspinous ligament
21 Thoracic spinal cord
22 Retrospinal fatty triangle (epidural fat)
23 Esophagus
24 Spinalis thoracis muscle
25 Spinal ganglion
26 Multifidus muscle
27 Accessory hemiazygos vein
28 Longissimus thoracis muscle
29 Left pulmonary artery
30 Costotransverse ligament (lateral)
31 Ligamentum flavum
32 Fifth rib (tubercle)
33 Superior articular process T5
34 Trapezius muscle
35 Inferior articular process T4
36 Iliocostalis thoracis muscle
37 Descending aorta
38 Fifth rib (body)
39 Transverse process T5

Figure 5. T2W axial image at the level of T4-5 disc space[8].

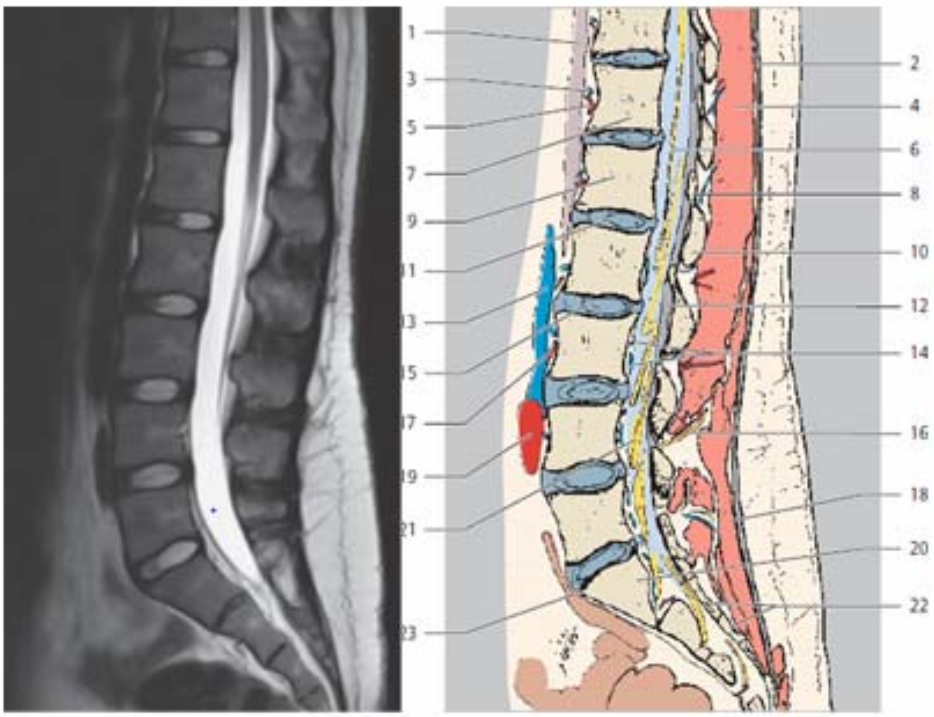

1 Spinal cord
2 Conus medullaris
3 Abdominal aorta
4 Ligamentum flavum
5 Lumbar vertebral body L1
6 Spinous process L1
7 Intervertebral disk L1/L2 (nucleus pulposus)
8 Interspinous ligament
9 Anterior longitudinal ligament
10 Supraspinous ligament
11 Intervertebral disk L2/L3 (annulus fibrosus)
12 Cauda equina
13 Basivertebral vein
14 Epidural fatty tissue
15 Left common iliac vein
16 Posterior longitudinal ligament
17 Sacral canal
18 Thecal sac (lumbar cistern)
19 Promontory of sacrum
20 Dura mater
21 Sacrum (S1)
22 Median sacral crest

Figure 6. T2W sagittal image through lumbosacral spine[8].

HISTORICAL BACKGROUND

The clinical field of MRI is comparatively new, yet its history spans more than a century and is renowned for several Nobel Prizes and key innovations in science and technology[9].

The study of MRI launched in 1882 with a major breakthrough in Physics: namely, the discovery of the rotating magnetic field by Nikola Tesla. In his honor, the "Tesla" became the international unit of magnetic flux density, which calibrates the strength of the magnetic field used in all MRI systems. Another breakthrough came more than a half century later in 1937, when Isidor Isaac Rabi from Columbia University successfully noted the magnetic instant of nuclei as well as the rotation of molecules, both key findings for the future of MRI. The research and development of nuclear (from spin nuclei) magnetic resonance spectroscopy was further cultivated by two scientists known as Felix Bloch of Stanford University and Edward Purcell of Harvard. In 1946, both Bloch and Purcell were successful in creating devices that could measure the magnetic resonance in matter. As a result of their accomplishment, they shared the 1952 Nobel Prize in physics for developing what is known as the foundation for nuclear magnetic resonance[9].

The field lagged for nearly 20 years before several advancements emerged during the early 1970s. First, Raymond Damadian of the State University of New York discovered a difference in relaxation times between normal and abnormal tissue (e.g., cancer)[9].

Damadian employed the origins of magnetic resonance developed from prior thought leaders and found a distinction in measured signals, known as spectroscopy. Around the same time, Paul Lauterbur utilized magnetic field gradients to produce the

first nuclear magnetic resonance images. The technique Lauterbur developed was termed Zeugmatography when published in 1973 in Nature, which illustrated magnet derived images of water-filled tubes[9].

The following year he published images of a clam, another first. While Lauterbur was creating two-dimensional images and lecturing, fellow scientist Peter Mansfield was working on improving the calculation used to process images in order to improve quality. Mansfield was successful and in 1978 presented the first cross-section images of both a finger and the abdomen[9].

Richard Ernst, a research scientist in Zürich, attended a lecture by Lauterbur in Raleigh and discovered a new reconstruction method for imaging. Ernst found that by altering the magnetic field, one could produce phase and frequency encoding, which continues to be the image reconstruction standard used today. While there were a great deal of accomplishments made by many individuals in the early 70s, in 2003 the Nobel Prize in Medicine or Physiology was shared by only two individuals — Lauterbur for the invention of MRI, and Mansfield for the continued improvements in imaging[9].

The final step towards advancing the clinical use of MRI was to build a magnet scanner, which was accomplished in 1977 and approved for clinical use by the Food and Drug Administration (FDA) in 1984. In addition, gadolinium, an MRI contrast agent, was patented and approved by the FDA four years later. Since FDA approval, clinical MRI has experienced continued global growth. Clinical MRI is a rather young field that has yielded extraordinary achievements[9].

Radiography of the spine began shortly after Roentgen's discovery in 1895. However, there was little written in the medical literature about spine imaging until nearly 25 years later with the development of myelography, first by using air and then a variety of positive contrast agents. The history of spine imaging before CT and MR imaging is, in large part, a history of the development of contrast agents for intrathecal use. The advent of CT and, more important, MRI revolutionized spine imaging. The spinal cord and its surrounding structures could now be noninvasively visualized in great detail. In situations in which myelography is still necessary, advances in contrast agents have made the procedure less painful with fewer side effects. Evolution of spine imaging has led to less invasive techniques for the evaluation of the spine and its contents and has resulted in more rapid, more specific diagnosis, therapy, and improved outcomes[10].

Conventional myelography and post myelographic CT are associated with considerable radiation exposure, possible reaction to the contrast material, and risk of lumbar puncture. Although CT myelography is superior to conventional myelography in visualizing the nerve rootlets, because of axial imaging, it is difficult to detect the entire extent of the injuries[11].

MRI seems to be the ideal tool for spinal imaging as it is non-invasive, not associated with risk of radiation exposure or need for contrast study, and provides excellent images of the thecal sac with soft-tissue contrast[11].

COMPRESSIVE MYELOPATHY

Compressive myelopathy refers to destruction of spinal cord tissue caused by pressure from degenerative spinal diseases/neoplasms/hematoma or other masses. Compressive disease is the main cause of myelopathy in older patients. It has a chronic course and usually does not recur[12].

Causes of Compressive Myelopathy

Causes of compressive Myelopathy are classified as shown in Table 1 [4,13].

Table 1. Causes for Compressive Myelopathy[4,13]

Spinal Neoplasms:	Extradural Neoplasms:	Tumors, cysts and tumor like masses	Neurofibroma
			Osteochondroma
			Vertebral body tumors
			Hemangioma
			Osteoclastoma
			Osteoblastoma
			Giant cell tumor
			Aneurysmal Bone cysts
			Epidural Lipomatosis
			Angiolipoma
			Synovial cysts
			Arachnoid cysts
			Malignant tumors
			Metastases
			Lymphoma
			Myeloma
			Sarcoma
			Chordoma
		Intradural / Extramedullary Neoplasms, Cysts and tumor like masses	Schwannoma
			Neurofibroma
			Meningioma
			Ganglioneuroma
			Paraganglioma
			Dermoid / Epidermoid
			Arachnoid cyst
			Lipoma
			Metastases
			Ependymoma.

	Intramedullary Tumors, Cysts and Tumor like masses		Ependymoma
			Astrocytoma
			Hemangioblastoma
			Glioblastoma
			Metastases
			Hydrosyringomyelia
			Developmental tumors
Epidural abscess			
Epidural haemorrhage			
Cervical Spondylosis			
Herniated discs			
Post–traumatic compression by fractured/displaced vertebra or haematoma.			

Degenerative compressive myelopathy

Degenerative compressive myelopathy may be classified according to the compression site, as follows[14]:

1. Anterior (disc protrusion or posterior osteophytes).
2. Anterolateral (Luschka joints).
3. Lateral (facet joints).
4. Posterior (ligamentum flavum)

It may be caused by atlanto-axial instability, spinal canal stenosis due to cervical spondylolysis, cervical spinal fusion, myelomeningocele or epidural masses[14].

Spinal Cord tumors and tumor like Masses:

Spinal cord tumors and tumor like masses are classified by location into three categories[3]:

1. Extradural lesions (lesions of osseous spine, epidural space, and paraspinous soft tissues).
2. Intradural extramedullary lesions (lesions that are inside the dura but outside the spinal cord).
3. Intramedullary lesions (spinal cord tumors and cysts).

Extradural Tumors, Cysts and Tumor like masses:

General imaging hallmarks of extradural mass lesions are focal displacement of the thecal sac and its contents away from the mass. MRI scan clearly shows the dura draped over the mass. In some cases a crescent of displaced epidural fat can be seen capping the lesion. The objectives of MRI evaluation of spinal tumors in the epidural space are detection of vertebral body lesions, even if there is no suspicion of epidural impingement and delineation of possible thecal sac impingement[3].

Degenerative Changes as a Cause for Compressive Myelopathy

Globally, cervical spondylotic myelopathy (CSM) is a common cause for spinal cord impairment among the elderly. MRI analysis has a significant role to play in predicting surgical outcome in patients with cervical spondylotic myelopathy[15].

Cervical canal stenosis is an important cause for cervical myelopathy. There is a crude correlation between grade of stenosis and myelopathy. MRI not only is an excellent investigation for evaluation of cervical canal stenosis, it also provides excellent inter-observer agreement[16].

Degenerative changes of the spine may include disc desiccation, fibrosis, narrowing of disc space, diffuse bulging of annulus beyond disc space, osteophytes of vertebral apophyses, defects, and sclerosis of end plates. Disc tissue extending beyond the edges of the ring apophyses, throughout the circumference of the disc, is referred to as ‘‘bulging’’. The terms ‘‘bulge’’ or ‘‘bulging’’ refer to a generalized extension of disc tissue beyond the edges of the apophyses. Such bulging involves greater than 25% of the circumference of the disc and typically extends to a relatively short distance, usually less than 3 mm, beyond the edges of the apophyses. Herniation is broadly defined as localized or focal displacement of disc material beyond the limits of intervertebral disc space (>25% of peripheral zone on axial plane). Herniated discs may be classified as protrusion or extrusion, based on the shape of the displaced material. Protrusion is present if the greatest distance between the edges of the disc material presenting outside the disc space is less than the distance between the edges of the base of that disc material extending outside the disc space. The base is defined as the width of disc material at the outer margin of the disc space of origin, where disc

material displaced beyond the disc space is continuous with the disc material within the disc space. Extrusion is present when, in at least one plane, any one distance between the edges of the disc material beyond the disc space is greater than the distance between the edges of the base of the disc material beyond the disc space or when no continuity exists between the disc material beyond the disc space and that within the disc space. The latter form of extrusion is best further specified or subclassified as sequestration if the displaced disc material has lost continuity completely with the parent disc. The term migration may be used to signify displacement of disc material away from the site of extrusion[17].

A study done in 79 patients aged > 65 years evaluated the functional significance of anterior and posterior degenerative spondylolisthesis (anterolisthesis and retrolisthesis) of the cervical spine to elucidate its role in the development of CSM. A total of 24 patients (30%) had displacement of ≥ 3.5 mm (severe spondylolisthesis), 31 had displacement of 2.0-3.4 mm (moderate spondylolisthesis), and 24 had < 2.0 mm displacement (mild spondylolisthesis group). In patients with severe spondylolisthesis, 14 patients had anterolisthesis and 10 patients had retrolisthesis. Patients with severe spondylolisthesis had a high incidence (93%) of degenerative spondylolisthesis at C3-4 or C4-5 and significantly greater cervical mobility than those with mild spondylolisthesis. The degree of horizontal displacement and cervical mobility did not differ significantly between the anterolisthesis and retrolisthesis groups. Severe cord compression seen on T1W magnetic resonance imaging (MRI) scans and high-intensity spinal cord signals seen on T2W MRI scans corresponded significantly to the levels of the spondylolisthesis. It was concluded from the study that degenerative spondylolisthesis is not a rare

radiographic finding in elderly patients with CSM, which tends to cause intense cord compression that is seen on MRI scans[18].

A study was done in 26 patients to evaluate the surgical results and prognostic factors for patients with soft cervical disc herniation with myelopathy. The study showed a male predominance (male-to-female ratio 4:1). C5-C6 level was the most frequently involved level. Clinically, the most obvious signs were gait disturbance, variable degree of spasticity, and discomfort in chest and abdomen and hand numbness. MRI was the imaging modality used in addition to CT and radiography and showed central disc herniation in 16 cases and accompanying cord signal changes in four patients[19].

Degenerative cervical spondylytic myelopathy (DCM) is caused by degeneration of spinal axis and resultant spinal cord compression. This may progress resulting in functional decline and severe neurological impairment. Cervical spondylytic myelopathy constitutes a big chunk of nontraumatic spinal cord injuries in Japan (59%), US (54%), Europe (31%), Australia (22%) and Africa (4 to 30%). DCM is known to result from multifactorial etiology such as age-related degeneration of the facet joints, intervertebral discs, or vertebral bodies; hypertrophy of ligamentum flavun; and in some cases ossification of posterior longitudinal ligament (OPLL). Degenerative changes of cervical spine in a significant number of asymptomatic patients ranging from > 35% to about 87% in various studies. In one study it was also found that severe degeneration of discs was seen in > 33% of volunteers. Prevalence of OPLL has been seen in up to 4% of population. MRI is currently one of the most valuable tools available to differentiate DCM and other

causes of neurological dysfunction as it can detect anatomic changes of spinal axis and parenchymal abnormalities including neoplasms, demyelination plaques and syringomyelia. MRI can also visualize neural, osseous, and soft-tissue structures with high-resolution and also help to delineate degree of degeneration and canal stenosis[20].

Trauma

MRI is an excellent imaging modality for detecting and assessing severity of spinal trauma. Presence of cord hemorrhage, maximum bony canal compression, and cord edema have been considered as best predictors of baseline neurological status at presentation and baseline ASIA score and cord hemorrhage have been considered as best predictors for final neurological outcome, thus highlighting the role of MRI in trauma[21].

In comparison with CT, MRI detects more traumatic disc herniations, epidural haematomas and spinal cord abnormality, though it was less sensitive in the detection of posterior element fractures. MRI has the advantage of demonstrating the precise relationships of the spinal cord to the vertebral column or retropulsed fragments at the level of injury. Focally increased signal intensity on T2W probably represents edema while focal hypointensity on long echo time images is consistent with the presence of deoxyhemoglobin. The incidence of asymptomatic post-traumatic spinal epidural hematoma was greater than was previously recognized. They have been reported to occur in upto 41% of spine injuries. Spinal epidural hematoma occurs as the result of tearing of a portion of the epidural venous plexus with focal extravasation of blood into the anterior epidural space. Most epidural hematomas from closed trauma are found in association with other injuries, are relatively small in size, and are probably

not significant clinically. The imaging characteristics of epidural hematomas are variable as they depend on the oxidative state of the haemorrhage and the effects of clot retraction[22].

Three patterns of cord damage in acute spine injury patients have been defined:

1. Central haemorrhage which increased with time.
2. Central petechial hemorrhage resolving with time
3. Edema and contusion only.

The presence of cervical spinal cord hemorrhage has a potent negative effect on motor recovery and is especially devastating to lower extremity motor function. Injuries to spinal cord can be classified into three patterns:

- Pattern I (most common) intraspinal hemorrhage
- Pattern II - Spinal cord edema
- Pattern III - Combination of intraspinal hemorrhage and edema[23].

The edematous spinal cord has a greater potential for functional recovery than hemorrhagic tissue. Patients with low intensity on T2W images had a poor prognosis. Many factors affects prognosis. The degree of cord compression appears to be the most important factor. Some patients with severe cord compression who showed normal intensity on T1 and T2W images had a good prognosis. Most patients with abnormal intensity on T1W images had poor prognosis. Hyperintensity itself on T2W images seems non-specific. The intensity on T2W images is considered to be a useful sign for clinical follow-up. Hyperintensity decreases or disappears in patients with

good recovery, while hyperintensity was unchanged in patients with a subsequent poor prognosis[23].

In comparison with CT, MRI can detect more traumatic disc herniations, epidural haematomas and spinal cord abnormality, though it is less sensitive in the detection of posterior element fractures. MRI has the advantage of demonstrating the precise relationships of the spinal cord to the vertebral column or retropulsed fragments at the level of injury. Where subluxation is present, this is better assessed by MRI than CT. MRI also optimally distinguishes between impingement on the theca or cord by subluxed vertebrae or concurrent hematoma. Identification of the true extent of ligaments injury is important practically and may alert clinicians to the risk of instability and delayed spinal cord compression[23].

MRI can provide information on hemorrhage and length of edema, which increases ability of predicting outcome by 16 to 33% compared to initial clinical scores alone. MRI evaluation of spinal cord following spinal cord trauma provides supplemental prognostic information on recovery of motor function[24].

Infections

Contrast enhanced MRI is a good diagnostic tool and has a definite role to play in differentiation of tubercular and pyogenic spondylodiscitis[25].

A study reported that skeletal involvement in tuberculosis occurs mainly by hematologic dissemination. Onset is insidious with symptoms ranging from months to three years[26].

In tuberculous (TB) spondylitis the cortical definition of affected vertebrae is invariably lost in contradistinction to pyogenic spondylitis. T1W images usually show decreased signal from the affected vertebral marrow. On T2W images, an indiscriminate increase in signal intensity is noted from vertebrae, soft tissues and discs. Posterior elements may be involved. Extension of TB spondylodiscitis to the adjacent ligaments and soft tissues is frequent, varying from 55% to 96%. This extension usually occurs anterolaterally; rarely, it has been observed posteriorly in the peridural space. The para vertebral masses are characterized by a thick irregular enhancement on CT and MR. Contrast enhanced MRI studies are especially useful for characterizing TB spondylitis. Rim enhancement around intraosseous and paraspinal soft tissue abscess is more common than in other infection. The sizes of the paraspinal masses have been noted to be generally larger in TB than in pyogenic infection. Spinal TB represents 25-60% of cases of skeletal TB. Thoracolumbar junction is affected most commonly and is relatively infrequent in the cervical and sacral segments of spine. Neurologic abnormalities may be encountered as a result of spinal cord compression from abscess, granulation tissue and bone fragments, and ischemia of the cord /intramedullary granulomas[27].

Careful correlation of MRI findings with clinical findings and lab data is important in outcome prediction in patients with spinal epidural abscess[28].

A study was conducted in 100 patients to assess frequency of various causes of non-traumatic paraparesis and tetraparesis based on MRI findings. It was observed from the study that paraparesis was more common than tetrparesis. Also spinal cord compression (SCC) was seen in 72% of patients. Neoplastic compression, infective

spondylitis and non-compressive myelopathies were the main causes of paraparesis. Spondylotic myelopathy was the most common cause for tetraparesis. It was concluded that MRI is helpful to evaluate spinal cord compression[29].

Early diagnosis of spinal epidural abscess (SEA) can be challenging resulting in delayed treatment. The morbidity of SEA is high and its mortality ranges from 18-31% in modern series. MRI is considered as the preferred imaging modality in the evaluation of spinal epidural abscess and is at least as sensitive as myelography with CT[30].

Tumours

Presence of SCC in patients who have a known malignancy has a significant impact on further management. It is therefore necessary that an accurate diagnosis is made to know the exact cause of spinal cord compression in these cases. MRI is very effective in the work up of patients with metastatic compression of the spinal cord and cauda equina[31].

A study showed that myeloma, breast cancer, prostate cancer, lung cancer and lymphoma are often seen involving the spine or soft tissue in the epidural space. The average age of patient with metastatic epidural disease can range from 53 to 58 years[32].

Metastatic lesions are often destructive and lytic but can be sclerotic, especially in prostate cancer. MRI is extremely sensitive to detection of metastasis in the vertebral bodies or extradural space. The multiplicity of lesions is strong evidence

for a metastatic origin. However, in the case of single lesion, differentiation of a metastatic lesion from a primary tumor or from a lesion of another etiology can be difficult[33].

Spinal cord epidural metastasis (SEM), a common complication of systemic cancer has been seen with an increasing frequency. Prostate, breast and lung cancer are the most common offenders. Metastasis commonly arises in the posterior aspect of vertebral body with later invasion of epidural space. Pathophysiologically, vascular insufficiency is more important than direct spinal cord compression. The most common complaint is pain, and two thirds of patients with SEM have motor signs at initial diagnosis. Currently magnetic resonance imaging is the most sensitive diagnostic tool[34].

MRI of the spine for the early diagnosis of SCC may be considered useful in patients with extensive skeletal metastasis and back pain[35].

Gadolinium-enhanced MRI is highly important for surgical planning of spinal cord and cauda equina tumours[36].

Intradural tumors account for 10 to 20% of primary central nervous system (CNS) neoplasms in adults of which, about two thirds are extramedullary and, with rare exception, well circumscribed and histologically benign. The vast majority of intraspinal nerve sheath tumors are schwannomas (neurinoma/neurilemmoma) and neurofibroma. Most of these tumours are intradural and extramedullary. These tumors are seen most often in adults between the ages of 20 and 50 years. One sixth of the

tumors have a purely extradural location, one sixth have both an intra and extradural component (dumbbell), while remainder are purely intradural[37].

Schwannomas are predominantly located laterally and obliquely to the spinal cord and may have broad based towards the dura. Schwannomas may have an epidural extension through intervertebral foramen with a 'dumbbell' shape. On T1W images, these lesions appear hypo- to isointense and on T2 W images they appear hyperintense[38].

Spinal meningiomas are slow growing tumours, which are initially asymptomatic and become symptomatic with cord compression. MRI is the diagnostic tool of choice for diagnosis of meningiomas[39].

Meningiomas are the second most common intradural spinal tumor, next only to neurofibromas and account for approximately quarter of all primary spinal tumors. Women, usually between their fourth and fifth decades, account for approximately 80% of patients with spinal meningiomas. A review of six major case studies of spinal meningiomas that included 571 cases, showed a frequency of 17% for cervical, 80% for thoracic and 3% for lumbar tumours. Pediatric spinal meningiomas are exceedingly rare, associated with neurofibromatosis and have a somewhat more uniform distribution throughout the spinal axis. Rare extradural extension or purely extradural lesions have been reported to occur at a frequency of 3.5% to 15%. Classically, spinal meningiomas appear iso intense to the spinal cord on T1 and T2W imaging with intense homogeneous signal on post contrast administration[40].

An MRI study was performed in 31 consecutive intradural extramedullary spinal tumors with histopathological confirmation. In 13 patients myelography had been performed. The results showed neuroma (n = 14) and meningioma (n = 11) as commonest conditions. Other tumours were metastases (n =3), lipomas (n = 2) and ependymoma (n = 1). Intradural extramedullary location of tumors was accurately assessed by MRI in all patients where as it was seen in only 10 of 13 patients with myelography. The MRI diagnoses were in accordance with the histologic findings in nearly 3/4th of cases. Intradural extramedullary tumors characteristically showed compression of cord or cauda equina with widening of the subarachnoid space above and below the mass or outward displacement of epidural fat[41].

MRI facilitates in differential diagnosis of spinal neurinomas and meningiomas based on the specific MRI patterns[42].

Most frequent site of spinal meningioma is in thoracic region. A study has concluded that MRI is the best imaging technique for diagnosis of spinal cord meningiomas[43].

Aneurysmal bone cysts although typically occur in the posterior elements they can often expand secondarily into the pedicles and vertebral body. In these patients, neural canal encroachment is common. Additionally, it may cause cord compression and pathological fracture. These patients most common present with pain and swelling[44].

Spinal cysts can cause extradural mass effect. For example, it has been observed that synovial cysts (juxta articular) may be a rare cause of extradural mass effect and is nearly always associated with facet degeneration. MRI helps to define the origin of the cyst (example, periarticular). The cyst will be localized adjacent to or dorsal to ligamentum flavum. Cyst may have a thin, well-defined rim of signal void due to its fibrous nature, peripheral calcification and occasional hemosiderin deposition. The signal characteristics of cyst fluid contents may parallel those of CSF but demonstrate no fluid motion. Slight hyperintensity on T1W images has been described as the most common appearance (due to increased protein content). Occasionally, the cyst contents may appear intensely and homogeneously hyperintense on all sequences, thus suggesting hemorrhage within the cyst. Areas of signal void within the cyst may reflect calcification or may result from air bubbles having migrated from a vacuum facet joint – this finding on MRI is virtually pathognomonic for cyst. Congenital and acquired arachnoid cysts are uncommon but important neoplastic causes of extradural mass effect. Extradural arachnoid cysts (EACs) are CSF-filled out pouchings of arachnoid layer that protrude through a dural defect; 2/3^{rds} occur in the mid to low thoracic spine, 20% in the lumbosacral region and 9% at the thoracolumbar junction. Cervical EACs are uncommon. Secondary bony changes include widened interpedicular distance, scalloping of the vertebral bodies or pedicle thinning and erosion[45].

Dynamic MRI can detect cases of cord compression not seen in neutral position and was diagnostic in all cases of mobile atlantoaxial instability where mobility at this joint affects the treatment options. Dynamic MRI is extremely useful

for evaluating craniovertebral junction abnormalities and, in particular, cord compression[46].

Altered Cord Signal Intensity

In patients with cervical compressive myelopathy, the MRI finding of increased signal intensity has shown a correlation with surgical outcome. The study included a total of 104 patients with cervical compressive myelopathy who were treated with cervical expansive laminoplasty. Increased signal intensity was classified into 3 grades: Grade 0, none; grade I, light (obscure) and grade II, intense (bright). MRI finding of increased signal intensity was positive in 86 patients. Correlation between preoperative increased signal intensity on T2 weighted sagittal MRI with patient age, duration of disease, posterior Japanese Orthopedic Associate (JOA) score and postoperative recovery rate showed that increased signal intensity can be a predictor of surgical outcome, thus highlighting the role of MRI in cervical compressive myelopathy[47].

A prospective study was done in 74 patients to analyze whether high intramedullary signal and contrast enhancement in MRI are associated with postoperative prognosis in patients with cervical myelopathy. The study results showed that intramedullary signal change is a poor prognostic factor and the intramedullary contrast enhancement on preoperative MRI should be viewed as the worst predictor of surgical outcomes in cervical myelopathy. Contrast enhancement and postoperative MRI are useful for identifying the prognosis of patients with poor neurological recovery[48].

Spinal Cord Measurements

Papadopoulos et al evaluated 42 patients with cervical compressive myelopathy who underwent decompressive surgery and its outcome based on ratio of anteroposterior-to-transverse diameter (RAPT) and presence of cord signal changes on MRI. Following surgery, if the cord was free of any impingement or effacement, it was considered as complete decompression. They classified patients into three groups based on presence of absence of cord signal changes (type 0 if there were no cord signal changes; type 1 if there is high-signal intensity in T2W imaging in one cord segment; and type 2 if ≥ 2 cord segments had signal changes). The mean preoperative cord compression ratios in the three groups were 49 ± 11% (group 0), 41.13 ± 12.62% (group 1), and 31.17 ± 9.1% (group 2). It was concluded from the study that intramedullary T2 signal changes do not necessarily herald poor prognosis. Patients with focal areas of high T2 signal changes in cord may have a similar prognosis as compared to patients without cord signal changes. However, multilevel involvement is indicative of a poorer course compared to the other two groups[49].

MATERIALS AND METHODS

Source of data:

This study is a descriptive observational study carried out in R. L. Jalappa Hospital, attached to Sri Devaraj Urs Medical College, over a period of 18months from January 2014 to June 2015 in 52 patients who were diagnosed with compressive myelopathy on MRI. Patients with symptoms of compressive myelopathy were referred for MRI of the spine at Department of Radio-Diagnosis. Patients were included in the study if they met the inclusion/exclusion criteria.

Inclusion Criteria:

All cases of compressive myelopathy diagnosed on MRI have been included in the study.

Exclusion Criteria:

Patients with contraindications for MRI studies were not considered for this study. These include patients with metallic implants and pacemakers; and claustrophobia.

Method of collection of data:

The study was conducted on all patients diagnosed with compressive myelopathy on MRI. Relevant clinical history of the patient was taken into account to know the symptomatology and the probable etiology. Detailed history for contraindication of MRI was taken before the MRI study. An informed consent was

taken from the patient for their willingness to participate in the study. MRI of spine was performed with 1.5 Tesla MRI scanner (Siemens® Magnetom Avanto®). Dedicated matrix spine coil for cervical, thoracic and lumbar spine was used for acquisition of images.

The following sequences were performed:

1. T2 weighted sagittal whole spine composition,
2. T1 weighted sagittal whole spine composition,
3. T1 weight axial images of relevant segment of spine,
4. T2 weighted axial images of relevant segment of spine,
5. Coronal short tau inversion recovery (STIR) sequences of region of interest,
6. T1 Fat saturation Sagittal whole spine composition,
7. T1 Fat saturation axial images of relevant segment of spine

Contrast MRI study (I.V gadolinium injection) was performed in some cases as required. Normal blood urea and serum creatinine results were confirmed prior to contrast-enhanced study.

The MRI findings have been analyzed with regard to location and extent of lesion, effect of lesion on spinal cord and possible diagnosis. In patients who underwent surgery, MRI findings have been correlated with surgical and pathology findings.

Spinal cord anteroposterior diameter and transverse diameter were recorded at the level of cord compression. Ratio of anteroposterior (AP) diameter-to-transverse

(TR) diameter (RAPT) was calculated by formula: RAPT (%) = AP/TR X 100[50]. Same measurements were performed above or below the lesion at a normal level. The percentage reduction of RAPT at the abnormal segment was then calculated for each patient.

The data has been analyzed using descriptive analysis. An open-source statistical software (OpenEpi®) has been used for data analysis.

RESULTS

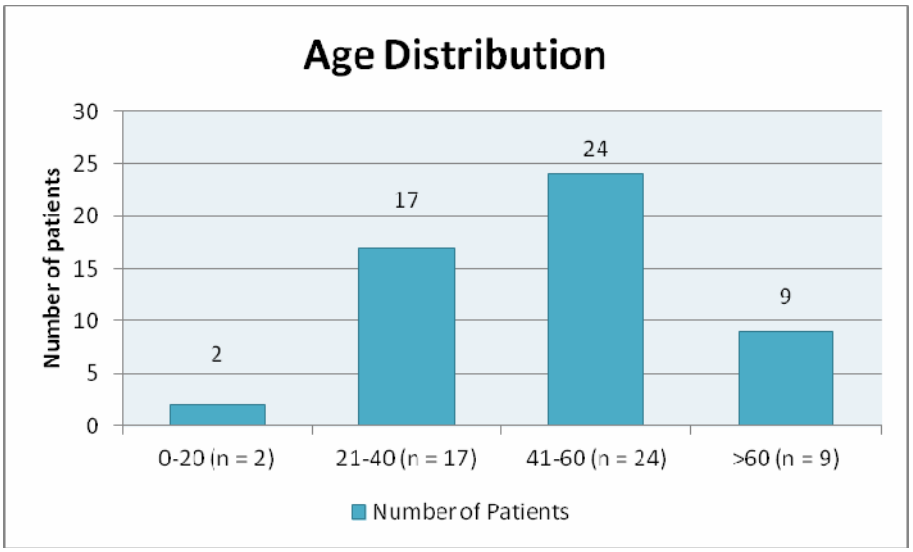

Figure 7. Age group distribution of patients.

Table 2. Age-group Distribution of Patients

Age group	Number of patients	%
0-20	2	3.8
21-40	17	32.7
41-60	24	46.2
>60	9	17.3

In our study, nearly half of the patients were in the age group of 41-60 years followed by 21-40 years which formed about 1/3rd of the patients (Figure 7).

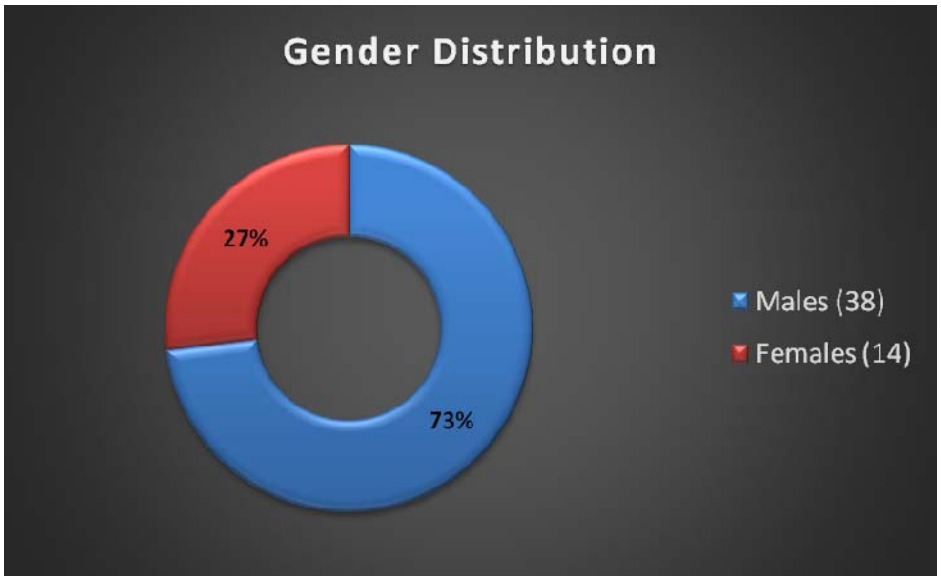

Figure 8. Gender-wise distribution of patients.

Table 3. Gender-wise Distribution of Patients

Gender	No of patients (%)
Male	38 (73%)
Female	14 (27%)

Men constituted nearly 3/4th of the patients (n = 38) (Figure 8).

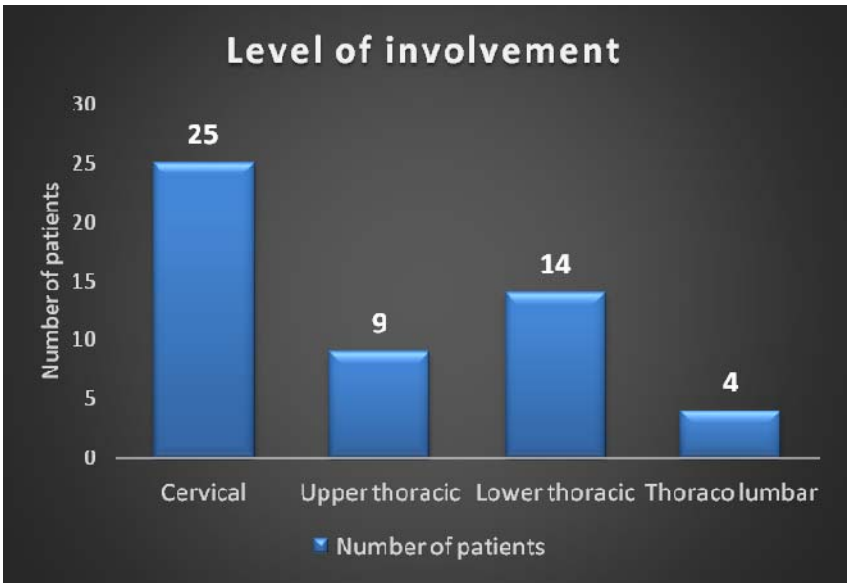

Figure 9. Level of spinal involvement

Table 4. Level of Spinal Involvement

Spinal Level Involvement	Number of patients
Cervical	25 (48%)
Upper thoracic	9 (17%)
Lower thoracic	14 (27%)
Thoraco lumbar	4 (8%)

Nearly half of the lesions were located in cervical spine (n = 25; 48%). Lesions in the lower thoracic spine were seen in 14 patients (27%), upper thoracic spine in nine patients (17%) and thoracolumbar spine in four patients (8%) (Figure 9).

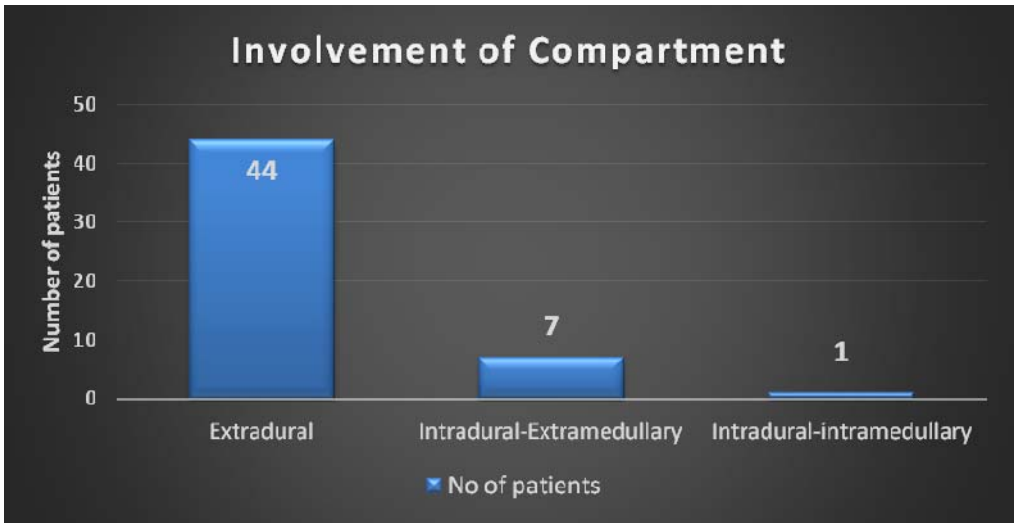

Figure 10. Involvement of various compartments.

Table 5. Involvement of Various Compartments

Compartment	No of patients
Extradural	44
Intradural-Extramedullary	7
Intradural-intramedullary	1

Approximately 85% of the patients (n = 44) had an extradural lesion. Intradural-extramedullary lesions were seen in seven patients (13%) and intradural-intramedullary lesion in one patient (2%) (Figure 10).

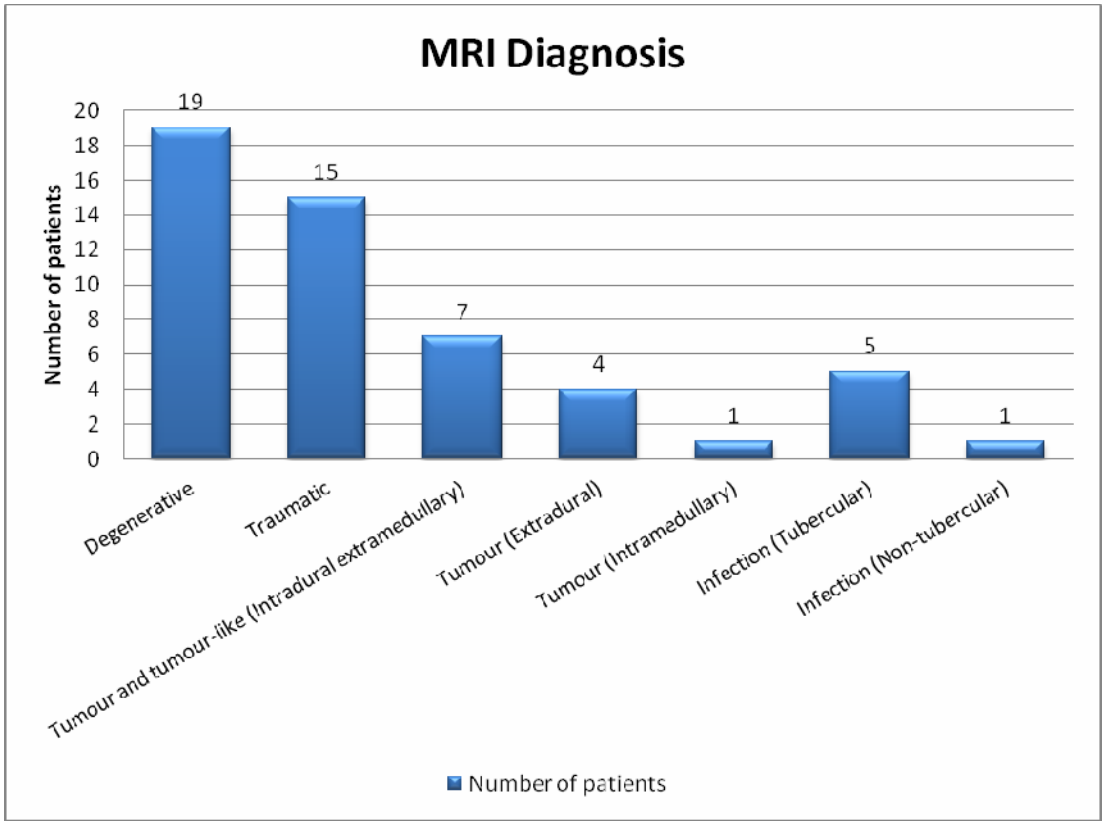

Figure 11. Causes for compressive myelopathy

Table 6. MRI Diagnosis of Various Causes of Compressive Myelopathy

MRI Diagnosis	Number of patients
Degenerative	19
Traumatic	15
Tumours and tumour-like (Intradural extramedullary)	7
Tumour (Extradural)	4
Tumour (Intramedullary)	1
Infection (Tubercular)	5
Infection (Non-tubercular)	1

The causes for compressive myelopathy were degenerative changes (n = 19; 36%), traumatic (n = 15; 29%), intradural extramedullary tumours and tumour-like (n = 7; 13.4%), extradural tumours (n = 4; 7.7%), intramedullary tumours (n = 1; 2%), tuberculosis of spine (n = 5; 9.6%), and non-tubercular infection (hydatid disease of spine) in one case (2%) (Figure 11).

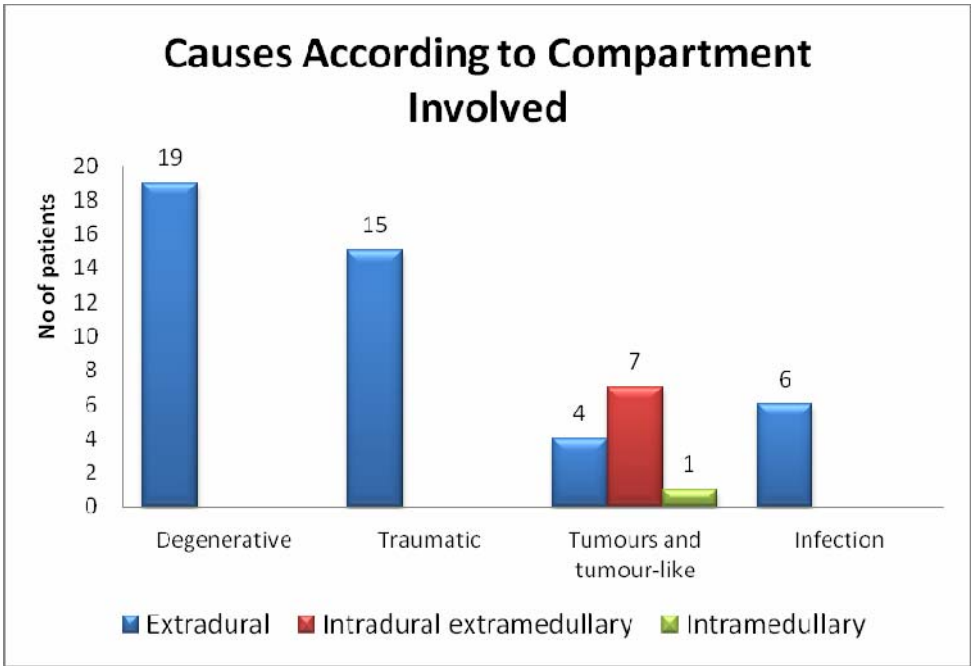

Figure 12. Causes of compressive myelopathy based on compartment involved.

Table 7. Causes of compressive myelopathy based on compartment involved

Cause	Extradural	Intradural extramedullary	Intramedullary
Degenerative	19 (36%)		
Traumatic	15 (29%)		
Tumours and tumour-like	4 (7.6%)	7 (13.4%)	1 (1.9%)
Infections	6 (12%)		

Extradural lesions were the commonest in our study (85%) followed by intradural extramedullary (13%) and lastly intradural intramedullary (2%).

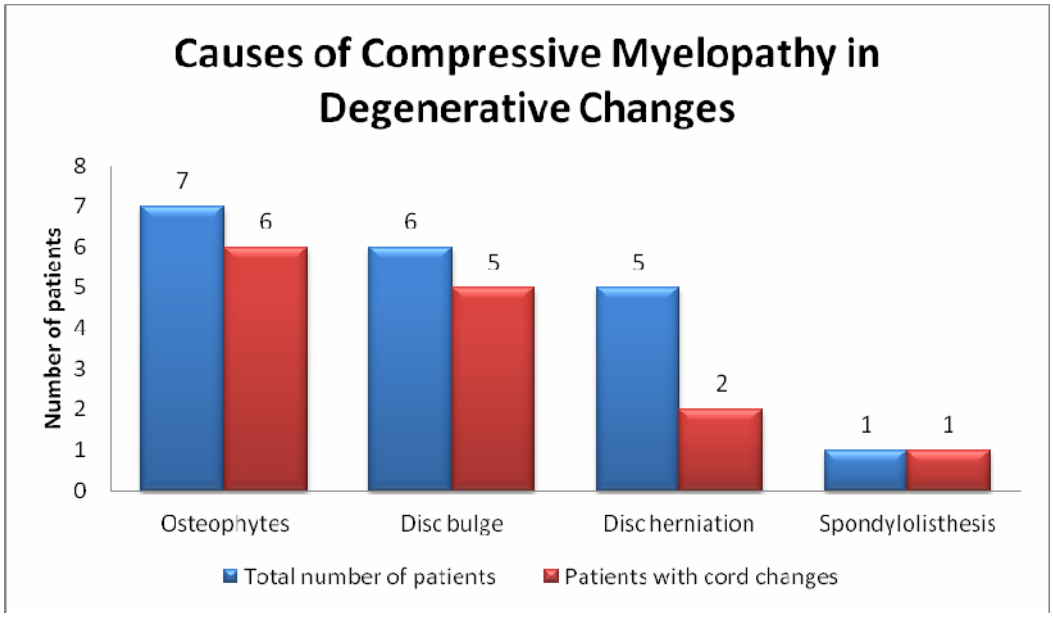

Figure 13. Causes of compressive myelopathy in degenerative changes.

Table 8. Causes of compressive myelopathy in degenerative changes.

Causes of myelopathy in degenerative changes	Total number of patients (in %)
Osteophytes	7 (36.8%)
Disc bulge	6 (31.5%)
Disc herniation	5 (26.5%)
Spondylolisthesis	1 (5.2%)
Total	**19 (100%)**

In our study all the cases of degenerative changes were seen in cervical spine (n = 19). Of these 73% of patients had cord signal changes (n = 14). The causes for cervical degenerative changes were osteophytes, disc bulges, disc herniations and spondylolisthesis (Table 8). In patients who had cord signal changes, osteophytes

were the commonest cause for cervical myelopathy (n = 6) followed by disc bulge (n = 5).

Degenerative changes were seen commonly in patients > 40 years (n = 14) and five patients in age group of 21-40 years had degenerative changes. The youngest patient with degenerative changes was 30 years and oldest patient was 75 years of age. Degenerative cervical myelopathy in the elderly (> 50 years of age) accounted for nearly half of all cases with cervical spine involvement (n = 10; 52%).

Osteophytes were in the form of uncovertebral osteophytes (n = 2) and disc osteophyte complex (n = 5). The levels involved were C3-4 (n = 4) and C4-5 (n = 3). Among six disc bulges three were diffuse disc bulges and remaining three were central with paracentral disc bulges. The levels involved were C5-6 (n = 3), C3-4 (n = 2) and C2-3 (n=1). Disc herniation was seen in five patients. Among them, three were central and paracentral disc protrusions; and two cases were disc extrusion with migration. The most common levels of compression were at C4-5 (n = 3), C3-4 (n = 2) and C5-6 (n = 1) levels. One patient had spondylolisthesis, at C6-7 level.

There were 15 cases of traumatic myelopathy – of these 12 were due to road traffic accidents (RTAs) and remaining three cases were due to fall from height.

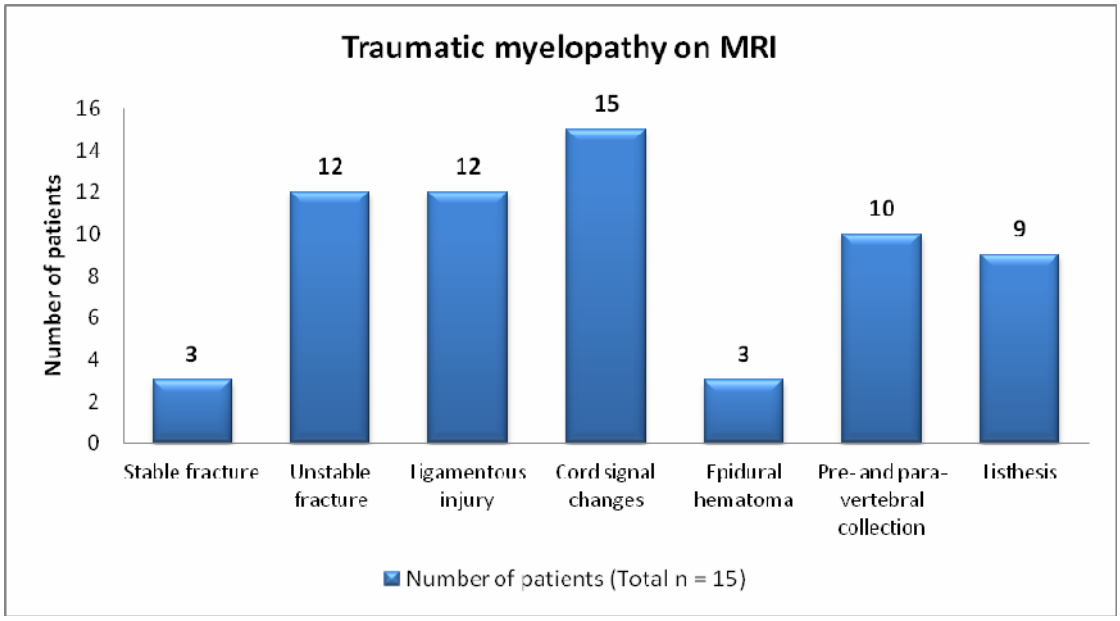

Figure 14. Characterization of traumatic myelopathy by MRI

Table 9. Characterization of Traumatic Myelopathy by MRI

Finding	**Number of patients (Total n = 15)**	**% involved**
Stable fracture	3	20%
Unstable fracture	12	80%
Ligamentous injury	12	53.3%
Cord signal changes	15	100%
Epidural hematoma	3	20%
Pre- and para-vertebral collection	10	66.7%
Listhesis	9	60%

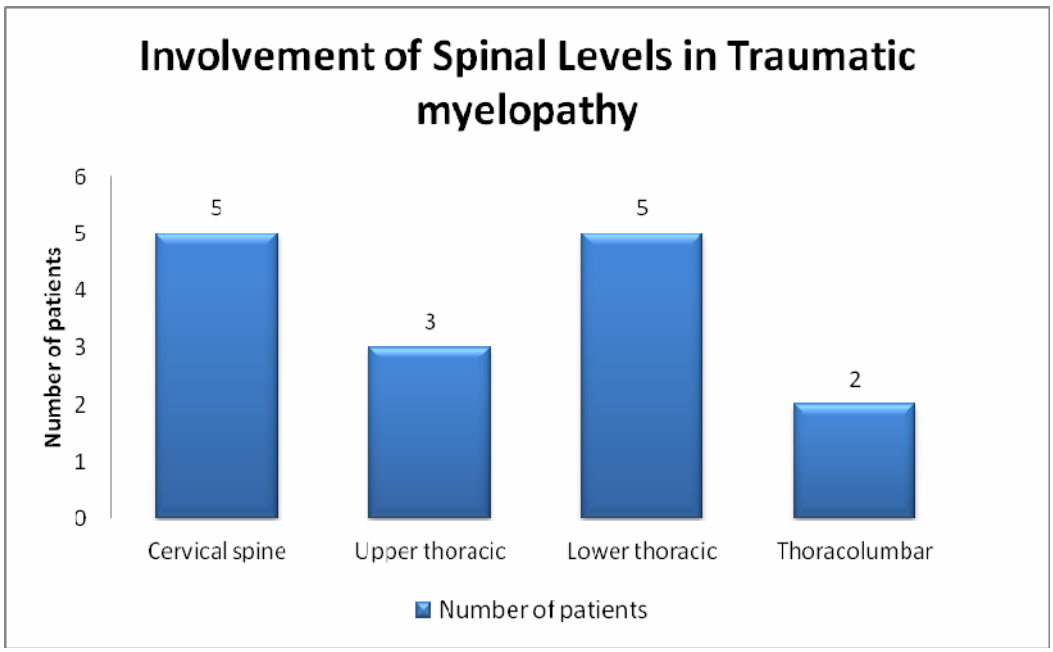

Figure 15. Involvement of spinal levels in traumatic myelopathy

Table 10. Level of Spinal Involvement in Traumatic Myelopathy

	Number of patient's n (%)
Cervical spine	5 (33.3%)
Upper thoracic	3 (20%)
Lower thoracic	5 (33.3%)
Thoracolumbar	2 (13.4%)

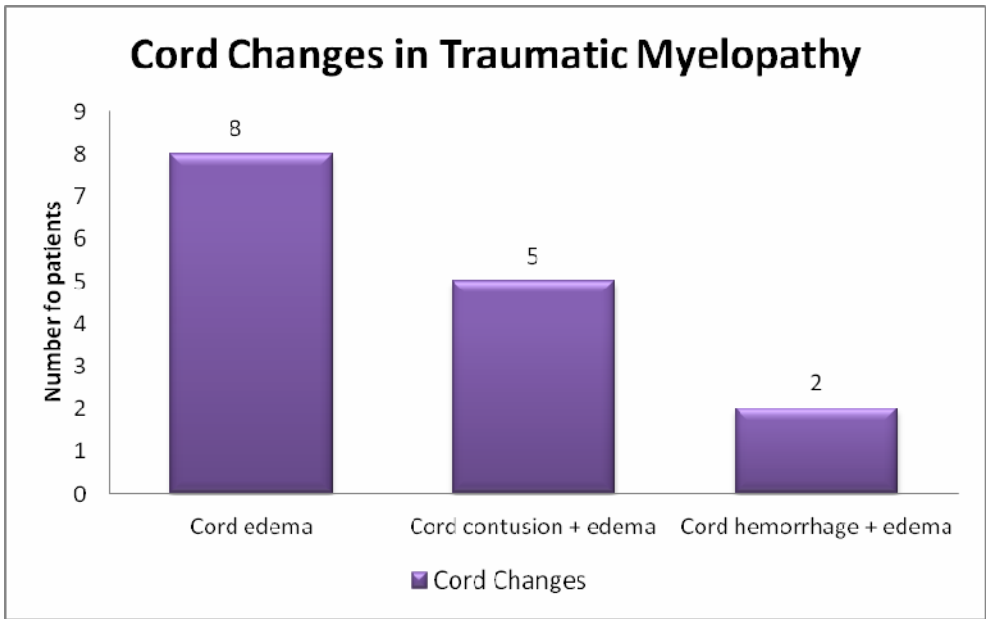

Figure 16. Cord changes seen in traumatic myelopathy

Cord changes were classified into three caterogies – cord edema, cord hemorrhage and cord contusion. Cord edema was seen as uniform high signal intensity on T2W images and normal signal intensity on T1W images. Cord hemorrhage was seen as low signal intensity on T2W images and heterogeneous signal intensity on T1W images within 24 hours of trauma and as heterogeneous signal intensity on T2W images between 48 hours to one week. Cord contusion was seen as area of intermediate-to-low signal on T2W images and normal signal intensity on T1W images. In our study, eight patients had only cord edema (53.3%), five patients had contusion with edema (33.3%), and two patients had cord hemorrhage with edema (13.3%) (Figure 16).

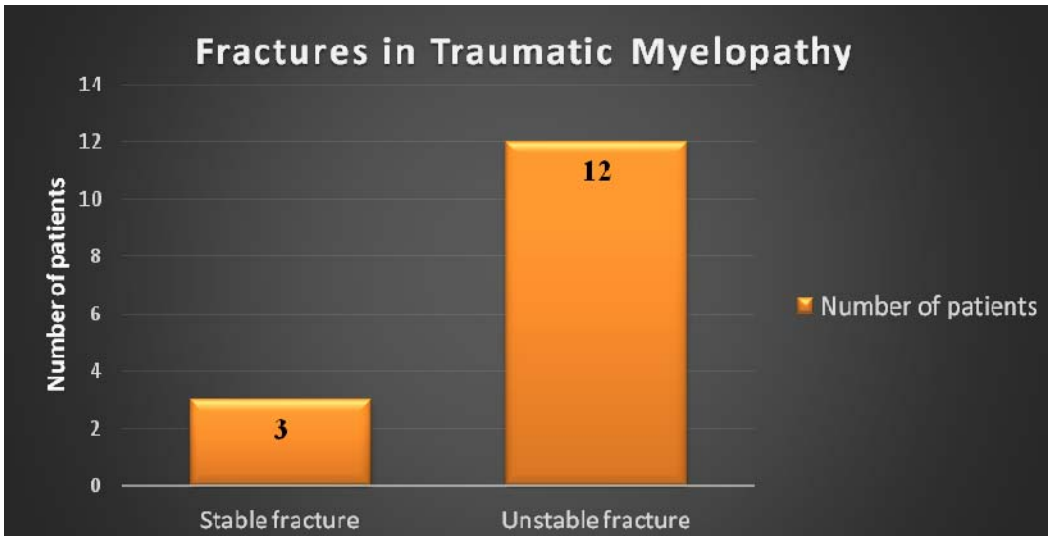

Figure 17. Spinal fractures – stable versus unstable

Table 11. Spinal Fractures – Stable versus Unstable

Type of fracture	Number of patients
Stable fracture	3
Unstable fracture	12

Fractures of the spine were classified into either stable or unstable fractures. A stable fracture was defined as fracture involving only anterior column resulting in anterior wedging of vertebral body and loss of anterior vertebral body height of less than 50%. An unstable fracture was defined was as a fracture involving disruption of two or more columns or involvement of posterior column or posterior element displacement and/or vertebral body or facet dislocation or subluxation[51].

All patients had spinal fractures of which 12 were unstable fractures (Figure 17). Listhesis was seen in nine patients, wedge compression in six patients, burst fracture in two patients and avulsion fracture in one patient.

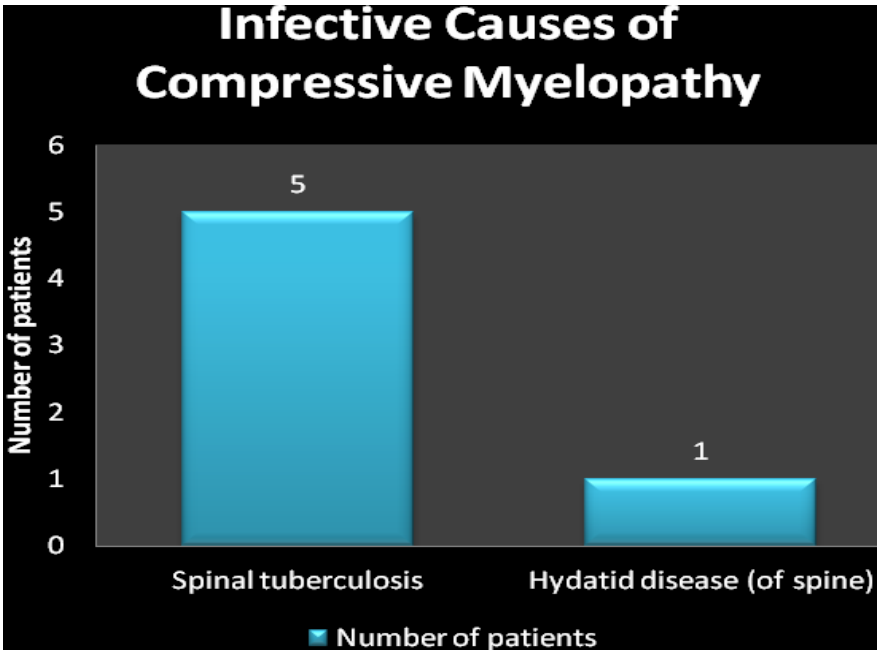

Figure 18. Infective Causes for Compressive Myelopathy

In our study, tuberculosis of spine was seen in five patients (9.6%) with age ranging from 25 to 58 years. There was a male predilection for tuberculosis of spine (n = 4; 80%). All the lesions were extradural and were seen in lower thoracic vertebral level. On MRI, two patients had kyphotic deformity, four patients had vertebral body collapse/anterior wedge compression, two patients had pedicle involvement, four patients showed partial collapse/destruction of disc, two patients had spondylodiscitis, all five patients had pre- and paravertebral collection and two patients had epidural cold abscesses. On contrast study, heterogeneous enhancement of the lesions was seen in all the five cases. Cord signal changes were seen in four patients (80%). One of the patients with epidural cold abscess did not have cord signal changes.

There was one case of hydatid disease of the spine, in a 33-year-old female patient. The disease involved T6 to T8 levels. MRI findings showed multiple cystic lesions in posterior to the vertebrae. A small intra spinal extra dural component was seen at T8 level, causing compression of the cord.

All cases of spinal tuberculosis and hydatid disease of the spine were correctly diagnosed on MRI and confirmed by cytology.

There were four cases of metastases of spine in our study (age ranging from 41 to 65 years) (Figure 19). The primary lesions were carcinoma prostate in two patients. One patient had carcinoma lung and other had carcinoma breast. Patients with metastasis from carcinoma lung and carcinoma prostate were males and the patient with carcinoma breast was a female patient. All the lesions were located in thoracic spine and were extradural. Cord signal changes were seen in all the four patients.

Eight patients with intradural tumours underwent surgery. There were seven intradural extramedullary mass lesions of which four cases were proved histopathologically to be neurofibromas. Of them one was correctly diagnosed on MRI. For two cases a differential diagnosis of neurofibroma and schwannoma was given and for the fourth case an additional differential diagnosis of meningioma was given.

There was one case of histologically proved meningioma for which a differential diagnosis of schwannoma was given on MRI.

There was one case of histologically proved schwannoma in which differential diagnosis of meningioma was given on MRI.

Arachnoid cyst was correctly diagnosed on MRI.

In the case of histologically proved astrocytoma, MRI differential diagnosis of astrocytoma and ependydoma was given.

In all the above mentioned cases, prior to surgery, the additional possibilities were mentioned considering age of the patient and MRI findings.

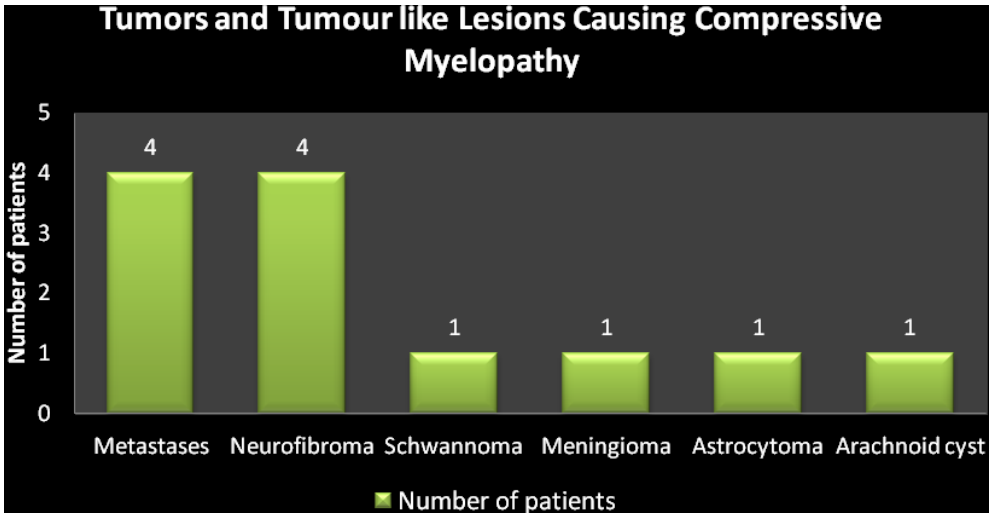

Figure 19. Tumors and tumour-like lesions causing compressive myelopathy.

Table 12. Location of Tumors and Tumour-like Lesions

Type of Tumour	**Location**
Metastases	Extradural
Neurofibroma	Intradural extramedullary
Schwannoma	Intradural extramedullary
Meningioma	Intradural extramedullary
Astrocytoma	Intramedullary
Arachnoid cyst	Intradural extramedullary

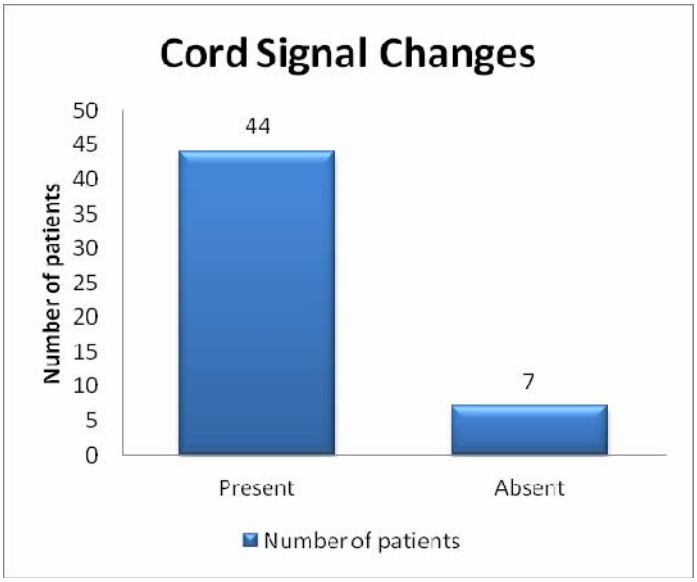

Figure 20. Presence of cord signal changes.

In the present study fifty one cases were extramedullary and one case was intramedullary. Cord signal changes were seen in 44 (86%) of the 51 patients with extramedullary lesions (Figure 20). Cord signal changes were seen at one level (n = 36), two levels (n = 2), three levels (n = 3), four levels (n = 2) and six levels (n = 1).

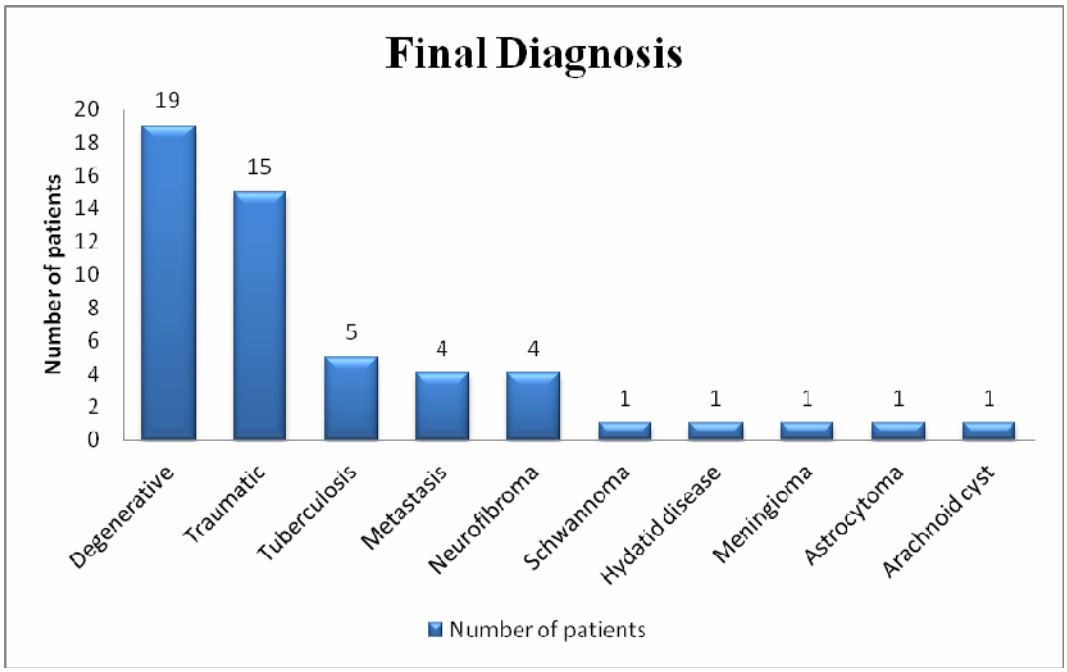

Figure 21. Final Diagnosis

Table 13. Final Diagnosis

Final Diagnosis	Number of patients
Degenerative	19
Traumatic myelopathy	15
Tuberculosis	5
Neurofibroma	4
Metastasis	4
Astrocytoma	1
Meningioma	1
Arachnoid cyst	1
Schwannoma	1
Spinal hydatid disease	1

Degenerative changes and traumatic myelopathy were the commonest diagnoses in our study (n = 19 and 15 respectively), followed by tuberculosis (n = 5), neurofibroma (n = 4), metastatic deposits (n = 4), astrocytoma, meningioma, schwannoma, arachnoid cyst and spinal hydatid disease (n = 1 each) (Figure 21).

Table 14. Signs and Symptoms Associated With Various Conditions

Diagnosis	Symptoms			Motor Changes	Sensory Changes
	Pain/ Radiculopathy	Weakness	Urinary incontinence	Paraparaesis	
Degenerative Changes	**19**	**11**	**-**	**-**	**19**
Traumatic myelopathy	**15**	**15**	**3**	**9**	**15**
Spinal tuberculosis	**5**	**1**	**-**	**4**	**4**
Metastases	**3**	**-**	**1**	**2**	**3**
Neurofibroma	**4**	**3**	**-**	**1**	**2**
Meningioma	**1**	**-**	**-**	**1**	**1**
Arachnoid cyst	**1**	**1**		**1**	**1**
Schwannoma	**1**			**1**	**1**
Astrocytoma	**1**	**-**	**-**	**-**	**1**
Hydatid disease of spine	**1**	**-**	**-**	**1**	**1**

Apart from the 15 cases of traumatic myelopathy, all patients demonstrated nonspecific signs and symptoms. Specific diagnosis of compressive myelopathy was made primarily after MRI.

The final diagnosis was correctly made in 46 of the 52 cases and a probable diagnosis was offered in the remaining 6 cases.

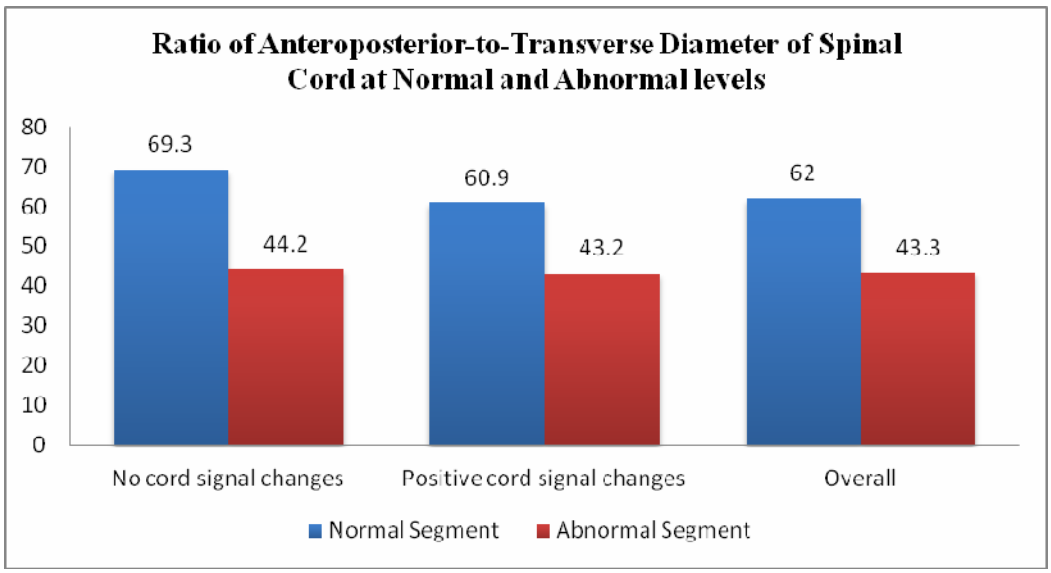

Figure 22. Ratio of Anteroposterior-to-Transverse Diameter of Spinal Cord in Normal and Abnormal Levels

Table 15. Ratio of Anteroposterior-to-Transverse Diameter of Spinal Cord in Normal and Abnormal Levels

	Ratio of anteroposterior-to-transverse diameter of spinal cord	
	Normal segment	Abnormal segment
No cord signal changes	69.3 (range 45 to 98.4)	44.2 (range 33.8 to 69.9)
Positive cord signal changes	60.9 (range 44 to 98)	43.2 (range 17.6 to 73.9)
Overall	62 (range 44 to 98)	43.3 (range 17.6 to 73.9)
	P = .37 (Uncorrected chi square)	

We compared the RAPT of spinal cord in normal and abnormal segments in patients who had abnormal T2 signal intensity in spinal cord and in patients who did not have abnormal T2 signal intensity. There was a reduction in RAPT in abnormal

cord segment by 33.5% ± 16% (mean ± SD) in patients who did not have cord signal changes and a reduction by 28.1% ± 23.6% (mean ± SD) in patients who had cord signal changes. Patients who had cord signal changes had lesser reduction in RAPT compared to patients who had no cord signal changes. This finding is contrary to what would be expected. Also the patients with no abnormal cord signals constituted only 13%. Overall there was mean reduction of 28.85% ± 22.8% (mean ± SD) in RAPT between normal and abnormal segments across all patients.

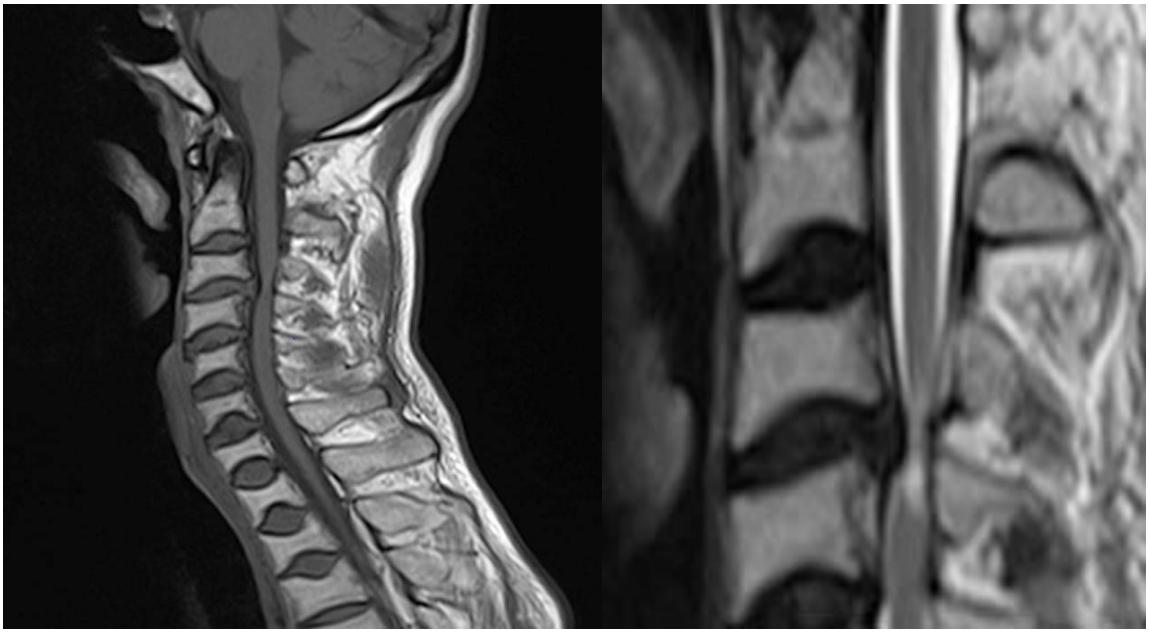

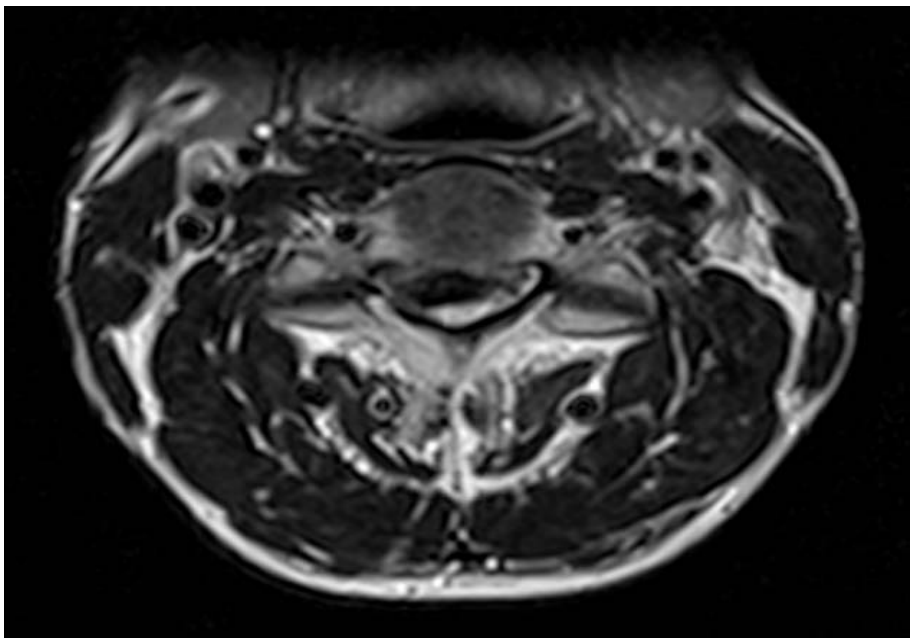

Figure 23 Case 38 Degenerative myelopathy showing central right paracentral disc herniation at C3-C4, obliteration of ventral thecal sac, cord compression and increased signal intensity in adjacent cord.

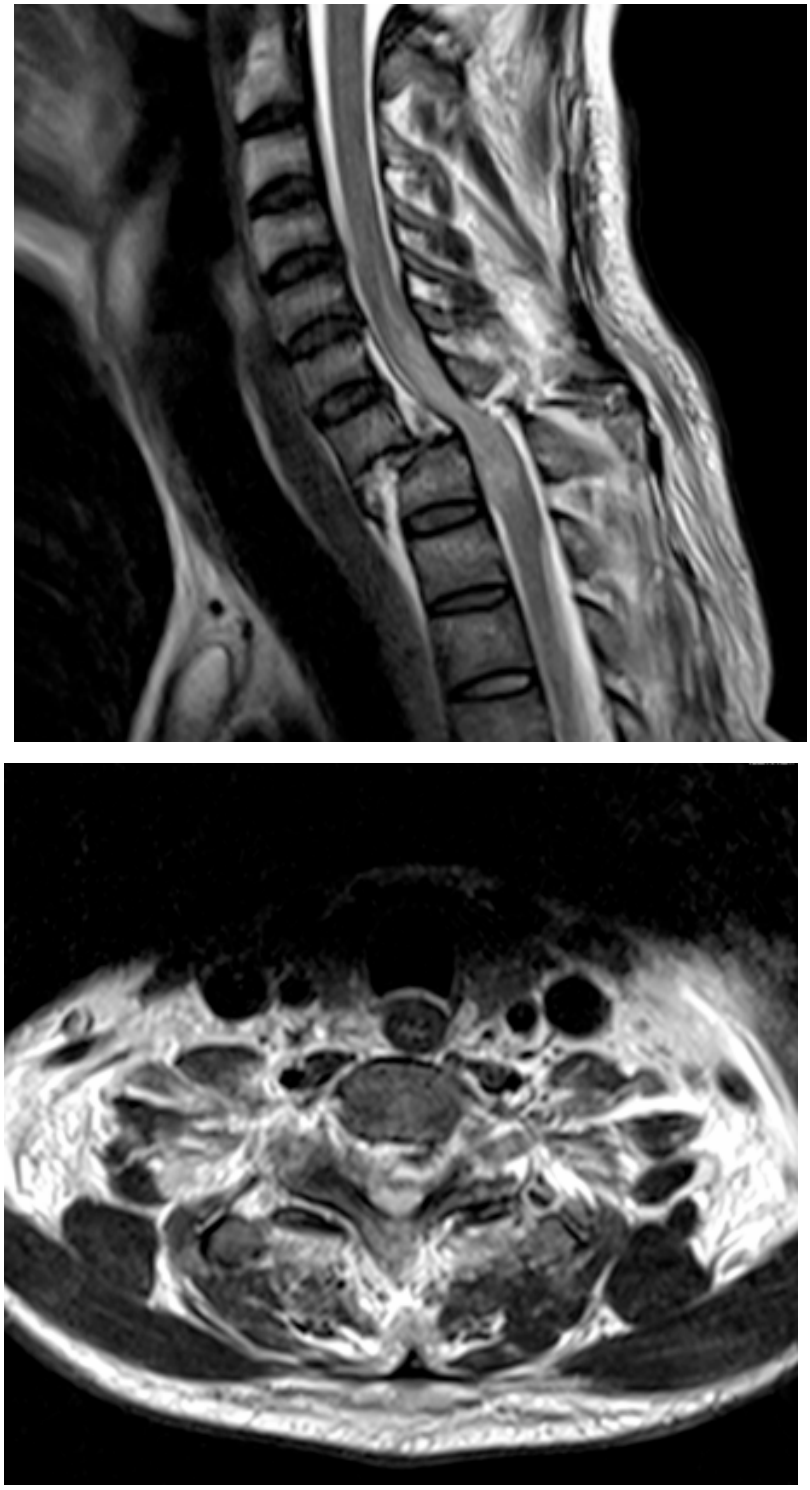

Figure 24 Case 47 A case of RTA showing grade III listhesis of C7 over T1 causing severe cord compression & edema involving three segments.

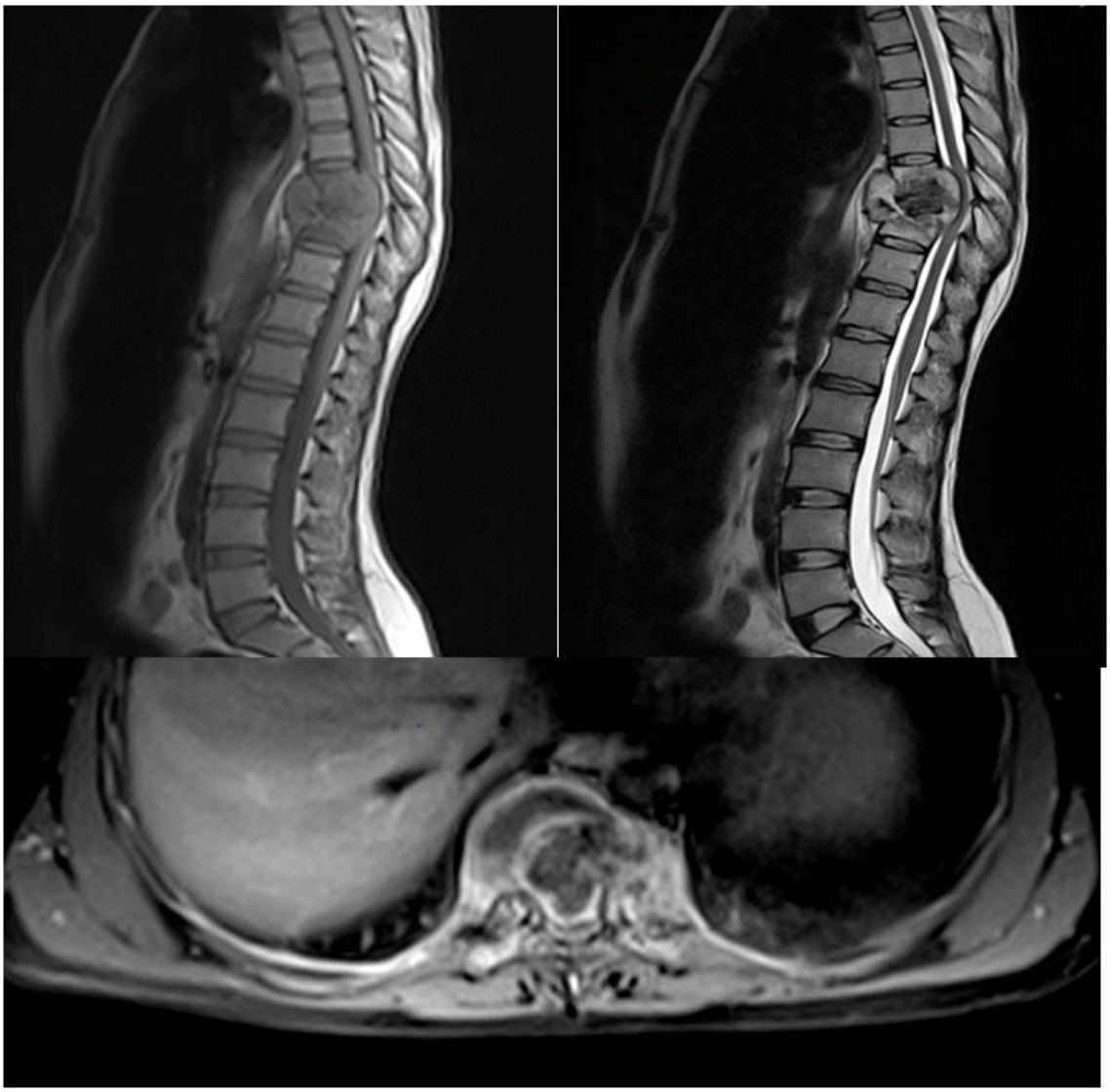

Figure 25 Case: 42 A case of Potts spine showing destruction of T8 and T9 vertebrae with formation of pre and bilateral para vertebral collection. Epidural collection causing cord compression (arrow).

Figure 26. Case: 7 A case of hydatid disease of spine showing multiple cystic lesions in the posterior spinal soft tissue. A small intra spinal cystic component (arrow) causing compression of the spinal cord.

Figure 27 Case: 34 A case of metastasis from prostate - there is extradural mass lesion at T6 level, posterior to the cord pushing the cord anteriorly and causing cord compression

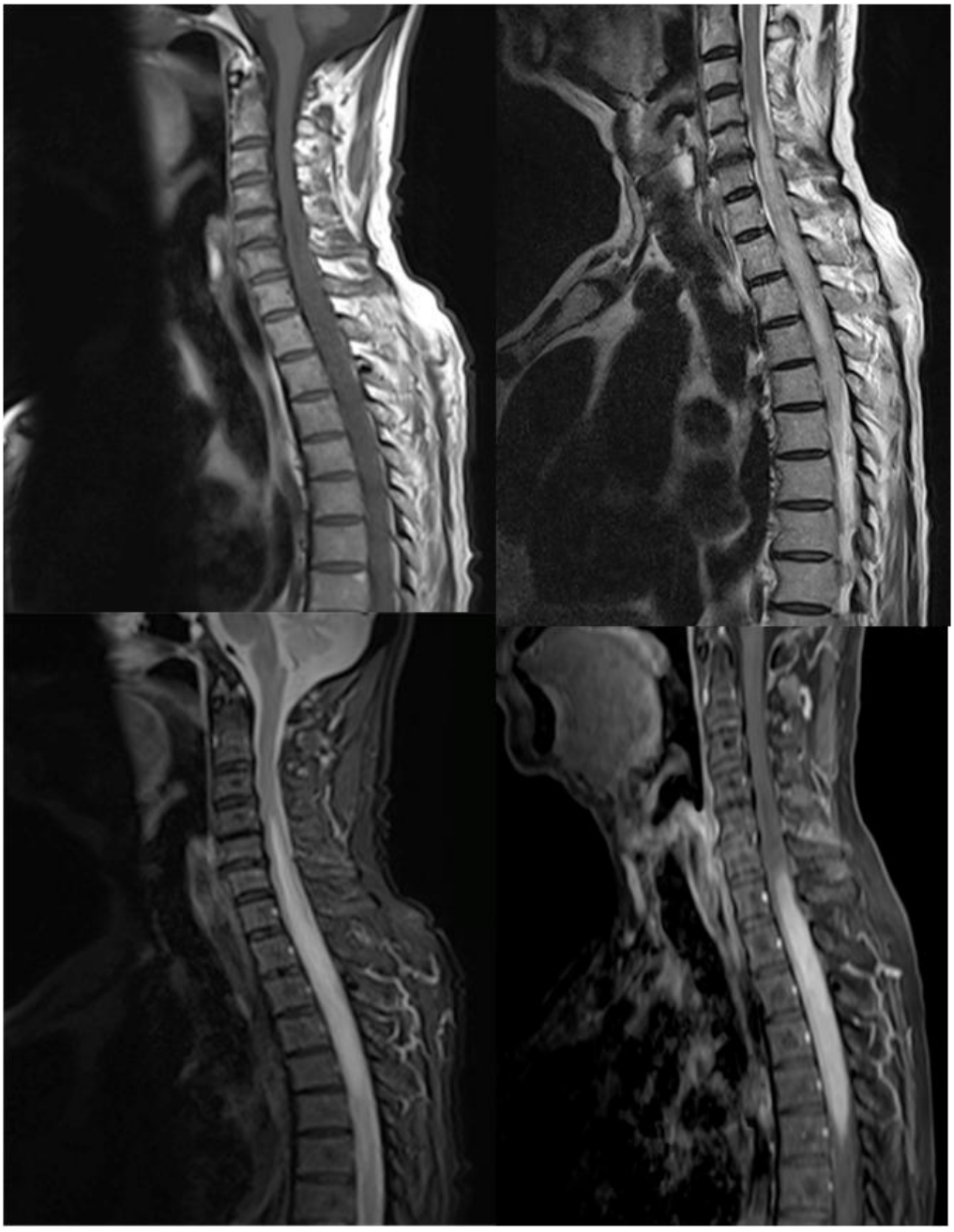

Figure 28 Case: 4 A case of astrocytoma –an expansile intramedullary fairly homogenous lesion in the spinal cord extending from C7 to T5 level causing effacement of the CSF space. Diffuse contrast enhancement noted within the lesion. Edema of the cord noted above and below the tumour.

Figure 29. Case 5 A case of arachnoid cyst - CSF signal intensity lesion in intradural, extramedullary space at T3 and T4 vertebral body levels in posterior thecal sac causing anteroposterior flattening and thinning of thoracic cord. Cord signal change seen extending up T7 vertebra.

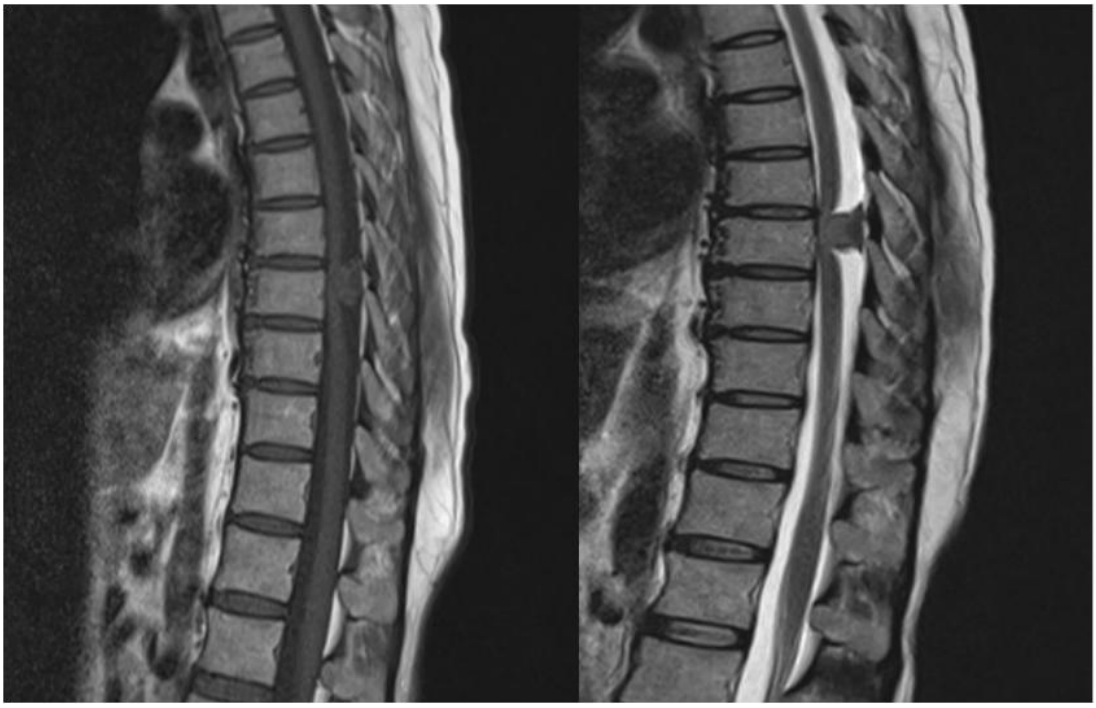

Figure 30. Case 20. A case of meningioma- A well circumscribed broad based extramedullary tumour at the level of T6-T7 causing anterior displacement of cord and compression at this level.

Figure 31 Case 2 A case of extramedullary Schwanomma- An intra dural extramedullary lesion which is extending from mid body of T2 till mid body of T4 vertebrae causing significant mass effect and compressing the spinal cord. On contrast administration there is homogeneous enhancement of mass lesion.

DISCUSSION

In our study of 52 patients the common age group was 41-60 years comprising 48% of patients (n = 24). Our results are in agreement with a recent study conducted by Diguvinti et al, who in their series of 25 patients found a similar age distribution of about 52% of cases in age group of 41-60 years[52].

Nearly 3/4th of the patients in the present study were males with a male-to-female ratio of 2.7:1. A similar male-to-female ratio of approximately 3:1 was seen in a study by Bhargwat Rai et al, which included 332 patients[53].

In the present study, 84.6% of the lesions were extradural in location, which is the commonest location of lesions[37,54].

The commonest cause in our study were degenerative changes (36%) followed by traumatic myelopathy (29%). The results from our study are in agreement with available literature, which suggest that degenerative changes are the commonest cause for myelopathy followed by trauma and extradural masses[2].

Degenerative Changes

All degenerative changes were seen in the cervical spine (n = 19). The common causes for degenerative changes were osteophytes (n = 7), disc bulges (n = 6) and disc herniations (n = 5) accounting for about 95% of all cases. Our results are in agreement with a review by Seidenwurm[2], where it has been mentioned that

cervical myelopathy caused by osteophyte or extruded disc of cervical spine is the commonest cause for myelopathy[2].

Globally, degenerative cervical myelopathy has been recognized as the commonest cause of spinal cord dysfunction[20].

Degenerative changes were seen commonly in patients > 40 years (n = 14; 73.7%). Degenerative cervical myelopathy in the elderly (> 50 years of age) accounted for nearly half of all cases (n = 10; 52%). Data from current literature shows that degenerative changes are more common in the elderly[15,16].

Traumatic Myelopathy

Traumatic myelopathy was seen commonly in the age groups of 41-60 years (n = 8 patients) followed by 21-40 years (n = 5). Only one patient older than 60 years had traumatic myelopathy. All but one patient were males (n = 14). Literature suggests that traumatic myelopathy is more common among males and is common in the younger age group[1]. Magu et al in their study of 57 patients found a male-to-female ratio of 2.8:1[55].

Road traffic accidents (RTAs) were the commonest cause for traumatic myelopathy accounting for about 80% of all cases of traumatic myelopathy (n = 12) in our study. Although, in literature RTAs have been reported to account for about 50% of cases of traumatic myelopathy[1], the higher incidence in our study is probably due to the close proximity of the hospital to a national highway.

In our study, there were five cases each of cervical spinal injury and lower thoracic injury (33.3%), three upper thoracic (20%) and two thoracolumbar injury (13.3%). Parizel et al have mentioned that approximately half of spinal injuries occur in the cervical spine[51]. The difference in incidence of cervical spine involvement may be attributed to different nature of trauma seen between developed and developing countries.

In our study, eight patients had only cord edema (53.3%), five patients had cord contusion with edema (33.3%), and two patients had cord hemorrhage with edema (13.4%). Our results are similar to study by Magu et al, who found that cord edema were seen in >70% of patients with traumatic myelopathy[55].

Ligamentous injury was seen in 12 patients (80%). In a study by Albrecht et al, it was observed that MRI is helpful in evaluation of extradural soft tissue/ligamentous injury. Of a total of 108 patients with normal radiograph in their study, MRI showed extradural soft tissue/ligamentous injury in 27 patients[56].

Infections of Spine

In our study, tuberculosis of spine was seen in five patients (9.6%) with age ranging from 25 to 58 years and a male predilection (n = 4; 80%). All the lesions were extradural and were seen in lower thoracic level.

In a review of 33 patients by Narlawar et al the age group for spinal tuberculosis ranged from 13 to 53 years, however, there was no significant gender predilection. Lower thoracic level was most commonly involved and was seen 48% of

cases followed by lumbar (39%) and cervical level (12%)[57]. In a review by Ansari et al, lower thoracic and lumbar vertebrae were the commonest sites involved in spinal tuberculosis[58].

On MRI, two patients had kyphotic deformity, four patients had vertebral body collapse/anterior wedge compression, two patients had pedicle involvement, four patients showed partial collapse/destruction of disc, two patients had spondylodiscitis, pre- and paravertebral collection in all five patients and two patients had epidural cold abscesses. On contrast study, heterogeneous enhancement of the lesions was seen in all the five cases. Cord signal changes were seen in four patients (80%). One of the patients with epidural cold abscess did not have cord signal changes.

Characteristic MRI findings described in tuberculosis of spine are destruction of two adjacent vertebral bodies and opposing end plates, destruction of intervening disc, vertebral body edema, presence of pre-, paravertebral and epidural abscesses and heterogeneous enhancement of vertebral body[58,59], one or more of which were seen in all our patients. A review by Ansari et al has shown that involvement of posterior elements in spinal tuberculosis is not uncommon and pedicles were the second most commonly involved in posterior element involvement[58].

There was one case of hydatid disease of the spine in our study, in a 33-year-old female patient. The disease involved from T6 to T8 vertebral levels. MRI findings showed multiple cystic lesions posterior to the vertebrae. A small intra spinal

extra dural component was seen at T8 level causing compression of the cord along with T2 hyper intensity.

Spinal hydatid disease is a rare condition seen in less than 1% of patients with hydatid disease. MRI features typically depict presence of multiple cysts (mother and daughter cysts is characteristic) in posterior vertebral and paravertebral region. Recurrence of hydatid cysts is known. Spinal hydatid disease has a poor prognosis[60,61].

Metastatic Lesions

There were four cases of metastases of spine in our study (age ranging from 41 to 65 years). The primary lesions were carcinoma prostate in two patients. One patient had carcinoma lung and another had carcinoma breast. Patients with metastasis from carcinoma lung and carcinoma prostate were males and the patient with carcinoma breast was a female patient. All the lesions were located in thoracic spine and were extradural. Cord signal changes were seen in all the four patients.

Chang and Lo have stated that thoracic spine is the commonest site for spinal metastasis. Vertebral column is the commonest site for bone metastasis in carcinoma breast, seen in up to 60% of cases[62]. Carcinoma lung is considered as the leading cause for metastatic cord compression in men followed by carcinoma prostate. Carcinoma prostate metastases are reported in 1 to 12% of cases of spinal metastasis[63].

Astrocytoma

In the present study there was one case of histologically proved astrocytoma, seen in a 65 year old male patient. The lesion was intramedullary and located in cervicothoracic region (C7 to T5 levels), showing hypointense signal on T1W images, hyperintense signal on T2W images and homogeneous enhancement on contrast study. For this patient, a differential diagnosis of ependydoma also was given.

Our patient profile is unlike the typical presentation of astrocytoma. Astrocytomas are typically seen in young patients (average age of presentation is 30 years) with more than half of the lesions seen in thoracic region, and no reported sex predilection[54]. Kim et al have shown that it is difficult to differentiate ependydoma and astrocytoma due to overlapping imaging features. These tumors usually show iso- to hypointense signal on T1W images and predominantly hyperintense signal on T2W images. Some astrocytomas may be non-enhancing, although some forms of astrocytomas can show heterogeneous enhancement. Diffuse enhancement has been observed more commonly in ependydoma compared to astrocytoma[64]. Considering the age and diffuse enhancement, an additional possibility of ependydoma was provided in this case.

Benign Lesions

There were four cases of histologically proved neurofibromas. On MRI, a differential diagnosis of schwannoma was given in two cases and one case had an additional differential diagnosis of meningioma. Patients with neurofibroma ranged from 19 to 37 years.

There was one case of histologically proved schwannoma in an 18 year old male patient. The lesion was hypointense on T1W images, hyperintense on T2W images and showed homogeneous enhancement on gadolinium administration. De Verdelhan et al in their review of 52 cases of schwannomas and meningiomas found that on MRI, schwannoma and meningioma have similar signal intensity on T1W images. However, on T2W images there is significantly hyperintense and heterogeneous signal. On contrast imaging a homogeneous enhancement is more likely to suggest meningioma[65]. Schwannomas are rare in younger patients[66]. In a large retrospective study by Conti et al involving 179 spinal neurinomas, it was found that the mean age group of involvement is 44 years and about 69% of these tumours are intradural[67]. Considering the age and atypical MRI findings, possibility of both schwannoma and meningioma was proposed.

Neurofibromas and schwannomas share similar MRI features, which include hypointense signal on T1W images, hyperintense signal on T2W images and enhancement following contrast administration. Both these tumours can have annular enhancements and irregular configurations and also have cystic degeneration[68].

In our study, there was one case of histologically proved meningioma, seen in a male patient aged 44 years. The lesion was located at T7-8 level. MRI finding included hypointense signal on T1W images, hyperintense signal on T2W images and homogeneous contrast enhancement. Considering the age and sex of the patient, possibility of meningioma or schwannoma was indicated.

Van Goethem et al in their review have stated that spinal meningiomas are seen more frequently in older individuals with a peak in 5th and 6th decade and with a female preponderance (females-to-males 70:30) and are most commonly located in thoracic spine. However, meningiomas in men tend to have uniform distribution in both cervical and thoracic spine[54].

There was one case of arachnoid cyst in a 50 year old female patient. The lesion was intradural extramedullary and showed hypointense on T1W images and hyperintense on T2W images (CSF signal intensity). The lesion was located at T3-T4 level.

Arachnoid cysts have typical MRI features which include hyperintense signal on T2W imaging and hypointense signal on T1W imaging. These cysts are believed to arise from herniation of arachnoid through congenital or acquired dural defects. These cysts are usually seen in mid-to-lower thoracic level and may protrude into the neural foramen[69].

MRI has been shown to accurately detect about 3/4th of intradural extramedullary cases in accordance to histologic findings. Intradural extramedullary tumours have been shown to characteristically have cord compression[41].

Cord Signal Changes

Cord signal changes were seen in 45 (86%) patients in our study including one patient with astrocytoma.

All 25 patients with cervical myelopathy showed obliteration of subarachnoid space. Twenty patients (80%) had cord signal changes. In the remaining five patients (20 %) who had no cord signal changes, the AP diameter of the affected cord was less than 9 mm. Our findings are similar to study by Matsumoto et al. In their study, out of 52 patients, increased signal intensity of spinal cord was seen in 34 patients (65%). Although, it is believed that increased cord changes are indicative of more severe disease, Matsumoto et al did not find any significant association between either increased cord signal intensity or spinal cord area in terms of outcome[70]. Overall there have been contrasting reports from various studies in terms of usefulness of considering cord signal intensity as a marker for outcome[71,72,73,74].

Out of 51 patients of extramedullary pathology 44 patients had increased cord signal changes. Changes were seen at one level (n = 36), two levels (n = 2), three levels (n = 3), four levels (n = 2) and six levels (n = 1).

Spinal Cord Measurements

In our study all but two patients had spinal cord anteroposterior diameter of < 10 mm at the site of pathology. In the two patients who had spinal canal diameter > 10 mm, there was obliteration of the subarachnoid space together with increased signal intensity of the cord.

Edward et al in their study of 63 patients have stated that in patients with symptomatic cervical spondylosis, an anteroposterior cervical spinal canal diameter of < 10 mm is indicative of myelopathy[75].

In our study, the mean RAPT was 43.3 (range 17.6 to 73.9) in abnormal spinal canal segments and 62 (range 45 to 98.4) in normal spinal canal segments. In patients with cord signal changes, the mean RAPT in abnormal spinal canal segments was 43.2 (range 17.6 to 73.9). In patients with no cord signal changes, the mean RAPT in abnormal spinal canal segments was 44.2 (range 33.8 to 69.9). There was an average reduction in RAPT in abnormal cord segment by about 33.5% ± 16% (mean ± SD) compared to normal cord segment in patients who did not have cord signal changes and an average reduction by about 28.1% ± 23.6% (mean ± SD) in patients who had cord signal changes on T2 weighted images. Patients who had cord signal changes had lesser reduction in RAPT compared to patients who had no cord signal changes. This finding is contrary to what would be expected. Also the patients with no abnormal cord signals constituted only 13%. Overall there was mean reduction of 28.85% ± 22.8% (mean ± SD) in RAPT between normal and abnormal segments across all patients. We have included RAPT in assessment as it can be considered a robust parameter. Ishikawa et al in their study of 229 patients have shown that RAPT is a robust parameter compared to other measurements such as transverse area of spinal cord or bony spinal canal diameter, which show age related changes[50].

Our results on RAPT reduction are similar to findings reported by Papadopoulos et al. They evaluated 42 patients with cervical compressive myelopathy who underwent decompressive surgery and its outcome based on RAPT and presence of cord signal changes on MRI. They classified patients into three groups based on presence of absence of cord signal changes (type 0 if there were no cord signal changes; type 1 if there is high-signal intensity in T1W images in one cord segment;

and type 2 if ≥ 2 cord segments had signal changes). The mean cord compression ratios in the three groups were 49 ± 11% (group 0), 41.13 ± 12.62% (group 1), and 31.17 ± 9.1% (group 2)[49].

Thus we see that a combination of morphological abnormalities, signal changes within the cord and objective measurements all contribute towards complete evaluation of compressive myelopathy.

CONCLUSION

In this study of 52 patients, extradural lesions were the commonest cause for compressive myelopathy. Cervical spine was the commonest location for compressive myelopathy. Degenerative changes were the commonest cause for compressive myelopathy followed by traumatic myelopathy.

All 25 patients with cervical myelopathy showed obliteration of subarachnoid space. Eighty percent of these patients had cord signal changes.

There was an average reduction of 28.85% ± 22.8% (mean ± SD) in the ratio of anteroposterior to transverse diameter between normal and affected segments.

Most of the patients demonstrated nonspecific signs and symptoms. Specific diagnosis of compressive myelopathy was made primarily after MRI.

MRI is a very effective modality in the diagnosis and evaluation of compressive myelopathy. Morphological abnormalities, signal changes within the cord and objective measurements all contribute towards complete evaluation of compressive myelopathy.

SUMMARY

The aim of the study is to evaluate various causes of compressive myelopathy and classify the lesions based on location into extradural and intradural compartments.

This is a descriptive observational study carried out over a period of 18 months from January 2014 to June 2015 in 52 patients who were diagnosed with compressive myelopathy on MRI. MRI of spine was performed with 1.5 Tesla MRI scanner (Siemens® Magnetom Avanto®).

Nearly half of the patients were in the age group of 41 to 60 years followed by 21 to 40 years. Men constituted nearly three quarters of the patients (n = 38).

Nearly half of the lesions were located in cervical spine (n = 25) followed by lower thoracic spine (n = 14; 27%), upper thoracic spine (n = 9; 17%) and thoracolumbar spine (n = 4; 8%). Approximately 85 % of the patients had extradural compression of the spinal cord, followed by intradural extramedullary (13 %) and intramedullary (2 %).

Degenerative changes (36%) and trauma (29 %) were common causes of compressive myelopathy. All the cases of degenerative changes were seen in cervical spine (n = 19). Of these 73% of patients had cord signal changes (n = 14) in the form of T2 hyper intense signal at the level of compression. Overall, osteophytes, disc bulges and disc herniations were the commonest causes accounting for majority of the cases (n = 18).

Cervical spine and lower thoracic spine were commonly involved in traumatic compressive myelopathy. Spinal cord changes were present in all the cases. Eight patients had cord edema (53.4%), five patients had cord contusion with edema (33.3%) and two patients (13.3%) had cord hemorrhage with edema.

Tuberculosis of spine was seen in five patients (9.6%) with a male predilection (n = 4; 80%). All the lesions were extradural and were seen in lower thoracic level. Cord signal changes were seen in four patients (80%). One of the patients with epidural cold abscess did not show cord signal changes. Other MRI features included kyphotic deformity, vertebral body collapse/anterior wedge compression, pedicle involvement, partial collapse/destruction of disc, spondylodiscitis, pre- and paraspinal collection and epidural cold abscess. There was heterogeneous enhancement of lesions post contrast administration.

Other conditions encountered in our study were metastasis and neurofibroma (n = 4 each), hydatid disease of spine, schwannoma, meningioma, astrocytoma and arachnoid cyst (n = 1 each).

Spinal canal anteroposterior diameter was <10 mm at the site of pathology in 50 patients. In the remaining two patients, although spinal canal diameter was > 10 mm, there was increased cord signal intensity along with obliteration of the subarachnoid space. In our study, the mean RAPT was 43.3 (range 17.6 to 73.9) in abnormal spinal canal segments and 62 (range 45 to 98.4) in normal spinal canal segments. In patients with cord signal changes, the mean RAPT in abnormal spinal

canal segments was 43.2 (range 17.6 to 73.9) with a reduction of 28.1% ± 23.6% (mean ± SD) compared to normal segments. In patients without cord signal changes, the mean RAPT in abnormal spinal canal segments was 44.4 (range 33.8 to 69.9) with a reduction of 33.5% ± 16% (mean ± SD) compared to normal segments. Overall there was mean reduction of 28.85% ± 22.8% (mean ± SD) in RAPT between normal and abnormal segments across all patients. RAPT is a robust parameter to evaluate cord compression compared to other measurements such as transverse area of spinal cord, which show age related changes.

Most of the patients demonstrated nonspecific signs and symptoms. Specific diagnosis of compressive myelopathy was made primarily after MRI.

MRI is a very effective modality in the diagnosis and evaluation of compressive myelopathy. MRI is helpful in depicting the changes within the spinal cord, assessing spinal cord lesions and adjacent pathology. It also helps to differentiate between spinal cord edema, contusion and hemorrhage in cases of trauma, which may have different prognostic implications for the patients. Morphological abnormalities, signal changes within the cord and objective measurements all contribute towards complete evaluation of compressive myelopathy.

BIBLIOGRAPHY

1 Sánchez AM, Posada LM, Toscano CA, Lopez AL. Diagnostic approach to myelopathies. Rev Colomb Radiol. 2011; 22:(3):1-21.

2 Seidenwurm DJ. ACR appropriateness criteria. Myelopathy. AJNR Am J Neuroradiol 2008;29:1032-4.

3 Osborn AG, editor. Cysts, Tumors and Tumor Like lesions of the spine and spinal cord. In diagnostic Neuroradiology. India: Mosby – Replika Press Pvt Ltd; 2003: 876- 905.

4 Thielen TV, van den Hauwe L, Van Goethem JW, Parizel PM. Imaging techniques and anatomy. In: Adam A, Dixon AK, Gilard JH, Schaefer-Prokop CM editors. Grainger & Allison's Diagnostic Radiology. 5th edition. Chapter 54. Churchill Livingstone Elsvier.2007 Pg: 1279-1294.e.1.

5 Blackham K, Sunshine JL. Spinal cord. In: Haaga JR, Dogra VS, Forsting M, Gilkeson RC, Ha HK, Sundaram M, editors. CT and MRI of the whole body. Chapter 17. 5th edition. Mosby Elsevier. 2003:Pg 733-54.

6 Kirsch C. The vertebral column and spinal cord. In: Butler P, Mitchell AWM, Ellis H, editors. Applied radiological anatomy for medical students. Chapter 11. 1st edition. Cambridge University Press. 2008:Pg 105-12.

7 Central nervous system. In: Butler P, Mitchell A, Healy JC, editors. Applied radiological anatomy. 2nd edition. Cambridge University Press. 2012:Pg: 82-8.

8 Spine. In: Moeller TB, Reif E, editors. Pocket Atlas of Sectional Anatomy. Computed Tomography and Magnetic Resonance Imaging. Volume III: Spine, Extremities, Joints. Thieme. 2007:Pg 263-315.

9 McCulloch ML. MRI Historical Background. Methodist Debakey Cardiovasc J 2009;5:13-4.

10 Hoeffner EG, Mukherji SK, Srinivasan A, Quint DJ. Neuroradiology Back to the Future: Spine Imaging. AJNR Am J Neuroradiol 2012;33:999 –1006.

11 Nakamura T1, Yabe Y, Horiuchi Y, Takayama S. Magnetic resonance myelography in brachial plexus injury. J Bone Joint Surg Br. 1997 Sep;79(5):764-9.

12 Ghezzi A Baldini SM, Zaffaroni M. Differential diagnosis of acute myelopathies. Neurol Sci 2001;22(Suppl 2):S60-4.

13 Diseases of the Spinal cord. Karper DL, Anthony SF, Longo DL, Braunwald E, Hauser SL, Jameson L. editors. In Harrison's principles of internal Medicine. Vol II, 16th Edition. MC Graw Hill companies, USA; 2004: 2440-1.

14 Montgomery DM, Brower RS. Cervical spondylotic myelopathy. Clinical syndrome and natural history. Orthop Clin North Am. 1992;23:487-93.

15 Nouri A, Tetreault L, Zamorano JJ, Dalzell K, Davis AM, Mikulis D, et al. Role of magnetic resonance imaging in predicting surgical outcome in patients with cervical spondylotic myelopathy. Spine (Phila Pa 1976). 2015 1;40:171-8.

16 Kang Y, Lee JW, Koh YH, Hur S, Kim SJ, Chai JW, et al. New MRI grading system for the cervical canal stenosis. AJR Am J Roentgenol. 2011;197:W134-40.

17 Fardon DF, Williams AL, Dohring EJ, Murtagh FR, Gabriel Rothman SL, Sze GK. Lumbar disc nomenclature: version 2.0: Recommendations of the combined task forces of the North American Spine Society, the American Society of Spine

Radiology and the American Society of Neuroradiology. Spine J. 2014 Nov 1;14(11):2525-45.

18 Kawasaki M, Tani T, Ushida T, Ishida K. Anterolisthesis and retrolisthesis of the cervical spine in cervical spondylotic myelopathy in the elderly. J Orthop Sci 2007;12:207-13.

19 Kim YJ , Oh SH, Yi HJ, Kim YS, Ko Y, Oh SJ. Myelopathy caused by soft cervical disc herniation : surgical results and prognostic factors. J Korean Neurosurg Soc 2007;42:441-5.

20 Tetreault L, Goldstein CL, Arnold P, Harrop J, Hilibrand A, Nouri A, et al. Degenerative cervical myelopathy: a spectrum of related disorders affecting the aging spine. Neurosurgery 2015;77 Suppl 4:S51-67.

21 Gupta R, Mittal P, Sandhu P, Saggar K, Gupta K. Correlation of qualitative and quantitative MRI parameters with neurological status: a prospective study on patients with spinal trauma. J Clin Diagn Res. 2014;8:RC13-7.

22 Hackney DB, Asata R, Sci DM, Joseph PM, Carvlin MJ, McGrath JT, et al. Hemorrhage and edema in Acute spinal cord compression. Demonstration by MR Imaging: Radiology 1986;161:387-390.

23 Kulkarni MV, McArdle CB, Kopanicky D, Miner M, Cotler HB, Lee KF, et al. Acute spinal cord injury: MR imaging at 1.5 T. Radiology 1987;164:837-43.

24 Flanders AE, Spettell CM, Tartaglino LM, Friedman DP, Herbison GJ. Forecasting motor recovery after cervical spinal cord injury: value of MR imaging. Radiology 1996;201(3):649-55.

25 Galhotra RD, Jain T, Sandhu P, Galhotra V. Utility of magnetic resonance imaging in the differential diagnosis of tubercular and pyogenic spondylodiscitis. J Nat Sci Biol Med. 2015;6:388-93.

26 LaBerge JM, Brant-Zawadzki M. Evaluation of Pott's disease with computed tomography. Neuroradiology 1984;26:429-34.

27 de Roos A, van Persijn van Meerten EL, Bloem JL, Bluemm RG. MRI of tuberculous spondylitis. AJR Am J Roentgenol 1986;147:79-82.

28 Numaguchi Y, Rigamonti D, Rothman MI, Sato S, Mihara F, Sadato N. Spinal epidural abscess: evaluation with gadolinium-enhanced MR imaging. Radiographics 1993;13:545-59

29 Ahmed N, Akram H, Qureshi IA. Role of MRI in differentiating various causes of non-traumatic paraparesis and tetraparesis. J Coll Physicians Surg Pak 2004;14:596-600.

30 Hlavin ML, Kaminski HJ, Ross JS, Ganz E. Spinal epidural abscess: a ten-year perspective. Neurosurgery 1990;27:177-84.

31 Li KC, Poon PY. Sensitivity and specificity of MRI in detecting malignant spinal cord compression and in distinguishing malignant from benign compression fractures of vertebrae. Magn Reson Imaging. 1988;6:547-56.

32 Han JS, Benson JE, Yoon YS. Magnetic resonance imaging in the spinal column and craniovertebral junction. Radiol Clin North Am 1984;22:805-27.

33 Smoker WR, Godersky JC, Knutzon RK, Keyes WD, Norman D, Bergman W. The role of MR imaging in evaluating metastatic spinal disease. AJR Am J Roentgenol 1987;149:1241-8.

34 Mut M, Schiff D, Shaffrey ME. Metastasis to nervous system: spinal epidural and intramedullary metastases. J Neurooncol. 2005;75:43-56.

35 Venkitaraman R, Sohaib SA, Barbachano Y, Parker CC, Khoo V, Huddart RA, et al. Detection of occult spinal cord compression with magnetic resonance imaging of the spine. Clin Oncol (R Coll Radiol) 2007;19:528-31.

36 Asazuma T, Toyama Y, Watanabe M, Suzuki N, Fujimura Y, Hirabayashi K. Clinical features associated with recurrence of tumours of the spinal cord and cauda equina. Spinal Cord. 2003;41:85-9.

37 Mc PC, Post KD, Stein BM. Intradural extramedullary tumors in adults. Neurosurg Clin N Am 1990;1:591-608.

38 Rothwell CI, Jaspan T, Worthington BS, Holland IM. Gadolinium-enhanced magnetic resonance imaging of spinal tumours. Br J Radiol 1989;62:1067-74.

39 Sandalcioglu IE, Hunold A, Müller O, Bassiouni H, Stolke D, Asgari S. Spinal meningiomas: critical review of 131 surgically treated patients. Eur Spine J. 2008;17:1035-41.

40 Bello JA. Radiologic imaging of intradural pathology. Neurosurg Clin N Am 1990;1:505-31.

41 Li MH, Holtås S, Larsson EM. MR imaging of intradural extramedullary tumors. Acta Radiol 1992;33:207-12.

42 Matsumoto S, Hasuo K, Uchino A, Mizushima A, Furukawa T, Matsuura Y, et al. MRI of intradural-extramedullary spinal neurinomas and meningiomas. Clin Imaging 1993;17:46-52.

43 Gezen F, Kahraman S, Canakci Z, Bedük A. Review of 36 cases of spinal cord meningioma. Spine (Phila Pa 1976) 2000;25:727-31.

44 Munk PL, Helms CA, Holt RG, Johnston J, Steinbach L, Neumann C. MR imaging of aneurysmal bone cysts. AJR Am J Roentgenol 1989;153:99-101.

45 Kochan JP1, Quencer RM. Imaging of cystic and cavitary lesions of the spinal cord and canal. The value of MR and intraoperative sonography. Radiol Clin North Am 1991;29:867-911.

46 Gupta V, Khandelwal N, Mathuria SN, Singh P, Pathak A, Suri S. Dynamic magnetic resonance imaging evaluation of craniovertebral junction abnormalities. J Comput Assist Tomogr. 2007;31:354-9.

47 Yukawa Y, Kato F, Yoshihara H, Yanase M, Ito K. MR T2 image classification in cervical compression myelopathy: predictor of surgical outcomes. Spine (Phila Pa 1976). 2007;32:1675-8.

48 Cho YE, Shin JJ, Kim KS, Chin DK, Kuh SU, Lee JH, Cho WH. The relevance of intramedullary high signal intensity and gadolinium (Gd-DTPA) enhancement to the clinical outcome in cervical compressive myelopathy. Eur Spine J. 2011;20:2267-74.

49 Papadopoulos CA, Katonis P, Papagelopoulos PJ, Karampekios S, Hadjipavlou AG. Surgical decompression for cervical spondylotic myelopathy: correlation between operative outcomes and MRI of the spinal cord. Orthopedics 2004;27:1087-91.

50 Ishikawa M, Matsumoto M, Fujimura Y, Chiba K, Toyama Y. Changes of cervical spinal cord and cervical spinal canal with age in asymptomatic subjects. Spinal Cord. 2003;41:159-63.

51 Parizel PM, van der Zijden T, Gaudino S, Spaepen M, Voormolen MHJ, Venstermans C, et al. Trauma of the spine and spinal cord: imaging strategies. Eur Spine J 2010;19 (Suppl 1):S8–S17.

52 Diguvinti S, Dara C. Clinico-MRI correlation of compressive myelopathy (restrospective study). Int J Appl Res 2015;1(7):60-4.

53 Rai B, Chopra BK, Raj Kumar. Spinal compression – An Analysis of 332 cases. J Assoc Physicians India 1971;19:647-51.

54 Van Goethem JWM, van den Hauwe L, Ozsarlak O, De Schepper AMA, Parizel PM. Spinal tumors. Eur J Radiol 2004;50:159-76.

55 Magu S, Singh D, Yadav RK, Bala M. Evaluation of traumatic spine by magnetic resonance imaging and correlation with neurological recovery. Asian Spine J 2015;9(5):748-756.

56 Albrecht RM, Kingsley D, Schermer CR, Demarest GB, Benzel EC, Hart BL. Evaluation of cervical spine in intensive care patients following blunt trauma. World J Surg. 2001;25:1089-96.

57 Narlawar RS, Shah JR, Pimple MK, Patkar DP, Patankar T, Castillo M. Isolated tuberculosis of posterior elements of spine: magnetic resonance imaging findings in 33 patients. Spine (Phila Pa 1976). 2002;27:275-81.

58 Ansari S, Amanullah MF, Ahmad K, Rauniyar RK. Pott's Spine: Diagnostic imaging modalities and technology advancements. N Am J Med Sci 2013;5:404-11.

59 Garg RK, Somvanshi DS. Spinal tuberculosis: A review. J Spinal Cord Med. 2011;34: 440–54

60 Prabhakar MM, Acharya AJ, Modi DR, Jadav B. Spinal hydatid disease: A case series. J Spinal Cord Med 2005;28:426–431.

61 Bhake A, Agrawal A. Hydatid disease of the spine. J Neurosci Rural Pract 2010;1:61–62.

62 Chang EL, Lo S. Diagnosis and management of central nervous system metastases from breast cancer. The Oncologist 2003;8:398-410.

63 Tazi H, Manunta A, Rodriguez A, Patard JJ, Lobel B, Guillé F. Spinal cord compression in metastatic prostate cancer. Eur Urol. 2003;44:527-32.

64 Kim DH, Kim JH, Choi SH, Sohn CH, Yun TJ, Kim CH, Chang KH. Differentiation between intramedullary spinal ependymoma and astrocytoma: comparative MRI analysis. Clin Radiol. 2014;69:29-35.

65 De Verdelhan O, Haegelen C, Carsin-Nicol B, Riffaud L, Amlashi SF, Brassier G, Carsin M, Morandi X. MR imaging features of spinal schwannomas and meningiomas. J Neuroradiol. 2005;32:42-9.

66 Kulkarni A, Srinivas D, Somanna S, Indira DB, Anathakrishna CB. Pediatric spinal schwannomas: An institutional study. J Pediatr Neurosci. 2012; 7:1–3.

67 Conti P, Pansini G, Mouchaty H, Capuano C, Conti R. Spinal neurinomas: retrospective analysis and long-term outcome of 179 consecutively operated cases and review of the literature. Surg Neurol 2004;61:34-43.

68 Gu R, Liu JB, Liu GY, Zhang Q, Zhu QS. MRI diagnosis of intradural extramedullary tumors. J Cancer Res Therap 2014;4:927-31.

69 Khosla A, Wippold II FJ. CT myelography and MR imaging of extramedullary cysts of the spinal canal in adult and pediatric patients. Pictorial Essay. AJR Am J Roentgenol 2002;178:201-7.

70 Matsumoto M, Toyama Y, Ishikawa M, Chiba K, Suzuki N, Yoshikazu F. Increased signal intensity of the spinal cord on magnetic resonance images in cervical compressive myelopathy. Does It Predict the Outcome of Conservative Treatment? Spine 2000;25:677–682.

71 Matsuda Y, Miyazaki K, Tada K, et al. Increased MR signal intensity due to cervical myelopathy. J Neurosurg 1991;74:887–92.

72 Morio Y, Yamamoto K, Kuranobu K, Murata M, Tuda K. Does increased signal intensity of the spinal cord on MR images due to cervical myelopathy predict prognosis? Arch Orthop Trauma Surg 1994;254–9.

73 Takahashi M, Yamashita Y, Sakamoto Y, Kojima R. Chronic cervical cord compression: Clinical significance of increased signal intensity on MR images. Radiology 1989;173:219–24.

74 Wada E, Ohmura M, Yonenobu K. Intramedullary changes of the spinal cord in cervical spondylotic myelopathy. Spine 1995;20:2226–32.

75 Edwards WC, LaRocca SH. The developmental segmental sagittal diameter in combined cervical and lumbar spondylosis. Spine (Phila Pa 1976) 1985;10:42-9.

ANNEXURE-I

PROFORMA

Name :

Age :

Sex :M ☐ F ☐

Chief Complaints :

Clinical diagnosis :

MRI Examination

Sequences :

TI :Iso ☐ Hypo ☐ Hyper ☐

T2 :Iso ☐ Hypo ☐ Hyper ☐

Post contrast :Enhancement ☐ No Enhancement ☐

STIR

Level of lesion / injury :

Number of Lesion :

Fracture : Stable / Unstable

Posterior Elements :

Compartment of compression :Extradural ☐ Intradural extramedullary ☐ ☐
intramedullary

Compression on the Cord :Present ☐ Absent ☐

Cord Changes :Present ☐ Absent ☐

Diagnosis :

Follow up :

ANNEXURE-II

INFORMED CONSENT FORM

I,

Mr/Miss/Mrs_____,

have been invited to participate in Research project titled "Role of Magnetic Resonanace Imaging in evaluation of extent and etiological factors in Compressive myelopathy". It has been communicated to me in my vernacular language about the purpose of the procedure and the associated possible complications.

My participation in this research project is purely voluntary. I am also aware that I can withdraw from the project at any point of time without citing any reasons whatsoever.

Hereby I give my consent by my own free will and in complete consciousness without any influence to participate and co-operate in the study.

Name and Signature/thumbprint.

Name and signature of third person

(In case the participant is illiterate or the patient is unconscious)

ANNEXURE-III

KEY TO MASTER CHART

-	Absent
#	Fracture
+	Present
↑	Hyperintense
↓	Hypointense
↔	Isointense
AC	Arachnoid cyst
AST	Astrocytoma
C	Cervical
DB	Disc bulge
Deg	Degenerative
DH	Disc herniation
E hem	Epidural hematoma
EC	Epidural cyst.
ECA	Epidural cold abscess
ED	Extradural
EPD	Ependymoma
EST	Epidural soft tissue
ESTM	Extramedullary soft tissue mass
F	Female
ID EM	Intradural Extramedullary
IM	Intramedullary
M	Male
MET	Metastatic

KEY TO MASTER CHART

MNG	Meningioma
NF	Neurofibroma
OST	Osteophytes
RP	Retropulsion
S#	Stable fracture
SCH	Schwannoma
SHD	Spinal hydatid disease
SL	Spondylolisthesis
STB	Spinal Tuberculosis
STI-T	Soft tissue intradural tumour
T	Thoracic
TM	Traumatic myelopathy
U#	Unstable fracture
VD	Vertebral displacement
VL	Vertebral lesion

MASTER CHART

SL. No	Hospital No	Age	Sex	Abnormal levels	Compartment	Morphology	Stable/Unstable Fracture	Cause of compression	Presence of Cord signal changes	Cord signal Changes	Cord signal changes >1 level	RAPT (Normal)	RAPT (Abnormal)	MR Diagnosis	Final Diagnosis
1	18181	40	M	C3-C4	ED	Pre- and paravertebral collection; listhesis	U#	VD	+	T2 ↓T1 ↔		**0.75**	**0.67**	TM	TM
2	19000	18	M	T2-T4	ID-EM	Extramedullary tumour	-	STI-T	+	T2 ↑ T1 ↓		**0.6**	**0.54**	SCH / MNG	SCH
3	34217	35	M	C4-C5	ED	Osteophytes	-	Ost	+	T2 ↑ T1 ↔		**0.54**	**0.41**	Deg	Deg
4	38683	65	M	C7-T5	IM	Intramedullary enhancing mass	-	STI-T	+	T2 ↑ T1 ↓	+	**0.67**	**1.67**	AST /	AST
5	44080	50	F	T3-T4	ID-EM	Extramedullary cystic mass	-	AC	+	T2 ↑ T1 ↓		**0.71**	**0.29**	AC	AC
6	45466	49	M	T4-T5	ED	Extradural soft tissue mass from carcinoma prostate	-	EST				**0.98**	**0.7**	Met	Met
7	47809	33	F	T6-T10	ED	Multiloculated cystic lesions	-	EC	+	T2 ↑ T1 ↔	+	**0.81**	**0.38**	SHD	SHD
8	71632	60	M	C4-5	ED	Osteophytes	-	Ost				**0.8**	**0.34**	Deg	Deg
9	93848	65	F	C3-C6	ED	Osteophytes	-	Ost	+	T2 ↑ T1 ↔	+	**0.54**	**0.36**	Deg	Deg
10	118029	49	F	C5-C6	ED	Disc bulge	-	DB				**0.45**	**0.4**	Deg	Deg
11	124977	60	M	T11-T12	ED	Listhesis	U#	VD	+	T2 ↓ T1 ↔		**0.75**	**0.22**	TM	TM
12	125730	42	M	T12	ED	Wedge compression fracture with retropulsion	S#	RP	+	T2 ↑ T1 ↔		**0.64**	**0.33**	TM	TM
13	126219	50	M	C5- C6	ED	Listhesis	U#	VD	+	T2 ↑ T1 ↔		**0.59**	**0.36**	TM	TM
14	128012	55	M	T12	ED	Wedge compression fracture with listhesis	U #	VD	+	T2 ↓ T1 ↔		**0.65**	**0.25**	TM	TM
15	131774	52	M	C5-C6	ED	Fracture with listhesis	U#	VD	+	T2 ↑ T1 ↔		**0.5**	**0.4**	TM	TM

MASTER CHART

SL. No	Hospital No	Age	Sex	Abnormal levels	Compartment	Morphology	Stable/Unstable Fracture	Cause of compression	Presence of Cord signal changes	Cord signal Changes	Cord signal changes >1 level	RAPT (Normal)	RAPT (Abnormal)	MR Diagnosis	Final Diagnosis
16	138349	70	F	T5-T6	ED	Listhesis	U#	VD	+	T2 ↑ T1 ↔		**0.58**	**0.23**	TM	TM
17	139871	41	M	T11-T12	ED	Epidural cold abscess, pre- and paraspinal collection, vertebral/disc collapse	-	ECA	+	T2 ↑ T1 ↓		**0.62**	**0.38**	STB	STB
18	141772	46	F	C2-5	ED	Osteophytes	-	Ost	+	T2 ↑ T1 ↔	+	**0.52**	**0.35**	Deg	Deg
19	145266	45	M	C6-C7	ED	Disc bulge	-	DB				**0.5**	**0.42**	Deg	Deg
20	145489	44	M	T7- T8	ID-EM	Enhancing extramedullary mass	-	STI-T	+	T2↑ T1 ↓		**0.66**	**0.37**	SCH / MNG	MNG
21	145676	19	M	T3-T4	ID-EM	Enhancing extramedullary mass	-	STI-T	+	T2 ↑ T1 ↔		**0.69**	**0.57**	SCH / NF	NF
22	156412	41	F	T6-T7	ED	Metastasis from primary carcinoma breast	-	ED mass	+	T2 ↑ T1 ↔		**0.75**	**0.63**	? Met	Met
23	148127	65	M	C4-6	ED	Disc bulge	-	DB	+	T2 ↑ T1 ↔	+	**0.58**	**0.36**	Deg	Deg
24	149043	68	M	C3-C4	ED	Disc herniation	-	DH	+	T2 ↑ T1 ↔		**0.5**	**0.36**	Deg	Deg
25	151665	23	M	T11-T12	ED	Wedge compression with retropulsion	S #	RP	+	T2 ↓ T1 ↔		**0.87**	**0.49**	TM	TM
26	156477	75	M	C2-C3	ED	Osteophytes	-	Ost	+	T2 ↑ T1 ↔		**0.51**	**0.35**	Deg	Deg
27	156980	37	F	T1-T2	ID-EM	Enhancing extramedullary mass	-	ESTM	+	T2 ↑ T1 ↓		**0.67**	**0.54**	SCH / NF / MNG	NF
28	160030	58	M	T8-T9	ED	Epidural cold abscess and paraspinal collection	-	ECA				**0.83**	**0.39**	STB	STB
29	164683	70	F	C3-C4	ED	Osteophytes	-	Ost	+	T2 ↑ T1 ↔		**0.45**	**0.38**	Deg	Deg

MASTER CHART

SL. No	Hospital No	Age	Sex	Abnormal levels	Compartment	Morphology	Stable/Unstable Fracture	Cause of compression	Presence of Cord signal changes	Cord signal Changes	Cord signal changes >1 level	RAPT (Normal)	RAPT (Abnormal)	MR Diagnosis	Final Diagnosis
30	164973	36	M	C4-C7	ED	Disc herniation	-	DH				**0.63**	**0.45**	Deg	Deg
31	165273	37	M	T7-T8	ED	Wedge compression with retropulsion	S #	RP	+	T2 ↑ T1 ↔		**0.66**	**0.62**	TM	TM
32	165713	50	M	C5-C6	ED	Epidural hematoma with listhesis	U#	EHem	+	T2 ↑ T1 ↔		**0.59**	**0.44**	TM	TM
33	195058	65	M	T11	ED	Epidural metastasis from carcinoma lung	-		+	T2 ↑ T1 ↔		**0.66**	**0.5**	Met	Met
34	517794	55	M	T6-T7	ED	Metastasis from carcinoma prostate	-	VL	+	T2 ↑ T1 ↓		**0.82**	**0.61**	Met	Met
35	933929	29	M	T10-T11	ED	Kyphosis, spondylodiscitis with vertebral body destruction, pre- and paravertebral collection	U#	EST	+	T2 ↑ T1 ↔		**0.7**	**0.54**	STB	STB
36	977498	35	M	C4-C7	ED	Disc herniation	-	DH	+	T2 ↑ T1 ↔	+	**0.5**	**0.34**	Deg	Deg
37	983576	40	M	T3-T4	ED	Burst fracture with retropulsion	U#	RP	+	T2↓ T1↔		**0.6**	**0.74**	TM	TM
38	985301	50	M	C3-C4	ED	Disc herniation	-	DH	+	T2 ↑ T1 ↔		**0.61**	**0.18**	Deg	Deg
39	987901	45	M	T11-T12	ED	Wedge compression with listhesis	U#	VD	+	T1↔ T2 ↓		**0.56**	**0.24**	TM	TM
40	988003	52	M	C5-C6	ED	Disc bulge	-	DB	+	T2 ↑ T1 ↔	+	**0.44**	**0.65**	Deg	Deg
41	988284	21	M	T11-T12	ED	Wedge compression with listhesis	U#	VD	+	T2↓ T1↔	+	**0.55**	**0.69**	TM	TM
42	990047	35	F	T9-T10	ED	Vertebral/disc collapse	-	EST	+	T2 ↑ T1 ↔		**0.79**	**0.72**	STB	STB
43	993521	42	F	C5-C6	ED	Osteophytes	-	Ost				**0.65**	**0.4**	Deg	Deg
44	994578	62	F	C6-C7	ED	Spondylolisthesis	-	SL	+	T2 ↑ T1 ↔		**0.48**	**0.34**	Deg	Deg

MASTER CHART

SL. No	Hospital No	Age	Sex	Abnormal levels	Compartment	Morphology	Stable/Unstable Fracture	Cause of compression	Presence of Cord signal changes	Cord signal Changes	Cord signal changes >1 level	RAPT (Normal)	RAPT (Abnormal)	MR Diagnosis	Final Diagnosis
45	1004106	30	M	T1-T2	ID-EM	Enhancing intradural extramedullary lesion.	-	STI-T	+	T2 ↑ T1 ↔		**0.6**	**0.38**	NF	NF
46	1004166	35	F	T2-T4	ID-EM	Enhancing intradural extramedullary lesion.	-	STI-T	+	T2 ↑ T1 ↓		**0.59**	**0.61**	NF	NF
47	1005331	48	M	C7-T1	ED	Avulsion fracture with listhesis	U#	VD	+	T2 ↑ T1 ↔	+	**0.46**	**0.33**	TM	TM
48	1015057	39	F	C3-C4	ED	Disc herniation	-	DH	+	T2 ↑ T1 ↔		**0.53**	**0.34**	Deg	Deg
49	108884	50	M	D12	ED	Burst fracture with # fragments causing cord compression	U#	#	+	T2 ↑ T1 ↔		**0.54**	**0.33**	TM	TM
50	107891	30	M	C5-C6	ED	Disc bulge	-	DB	+	T2 ↑ T1 ↔		**0.49**	**0.39**	Deg	Deg
51	112988	50	M	C5-C6	ED	Disc bulge	-	DB	+	T2 ↑ T1 ↔		**0.55**	**0.33**	Deg	Deg
52	146397	25	M	T10-T11	ED	Collapse/compression of vertebrae Pre and paravertebral collection	-	EST	+	T2 ↑ T1 ↔		**0.57**	**0.47**	STB	STB